



TURBOMACHINERY & PUMP SYMPOSIA | HOUSTON, TX  
**SEPTEMBER 26-28, 2023**  
SHORT COURSES: SEPTEMBER 25, 2023

**DESIGN AND ANALYSIS OF LARGE INDUCTION MOTORS FROM A MECHANICAL STANDPOINT**

**Jim Keck**

Senior Mechanical R&D Engineer  
TECO-Westinghouse  
Round Rock, Texas, USA

**Troy Feese**

Senior Staff Engineer  
Engineering Dynamics Incorporated  
San Antonio, Texas, USA



*Jim Keck is a Senior Mechanical R&D Engineer at TECO-Westinghouse Motor Company (TWMC). He has over 30 years of experience in the field of rotating equipment, including diesel-electric and large custom designed induction and synchronous motors and generators with ratings from 500 to 25000 HP and speeds from 180 to 15000 RPM. He has performed extensive study and analysis in rotordynamics, modal analysis, stress, ventilation, heat transfer, and bearing design. Jim received his BSME from LeTourneau University in Longview, Texas in 1989. He participated in the API 541 5<sup>th</sup> Edition committee and has been heavily involved with field-service and troubleshooting issues throughout his career. Jim has designed and tested many new motor designs and their related features and has his name on several patents in this field.*



*Troy Feese is a Senior Staff Engineer at Engineering Dynamics Incorporated (EDI). He has 32 years of experience performing torsional vibration, lateral critical speed, and rotordynamic stability analyses as well as evaluating structures using finite element methods. He conducts field studies of rotating machinery, reciprocating equipment, piping, structures, and foundations around the world. Mr. Feese received a BSME from The University of Texas at Austin in 1990, has a MSME from UTSA, is a licensed Professional Engineer in Texas, and is an ASME Fellow. He has contributed to the Vibration Institute, the GMRC torsional sub-committee, and an earlier version of API 684. He has authored technical papers on torsional vibration, lateral critical speeds, VFD motors, and field balancing. He has made presentations at the Turbomachinery Symposia, Gas Machinery Conferences, Torsional Vibration Symposia in Austria, and PCIC in Vancouver, Canada.*

**ABSTRACT**

This tutorial covers the following topics:

- Two-pole versus four-pole motors
- Complications with two-pole having higher speed, uneven magnetic forces, variable speed operation
- Review of American Petroleum Institute (API) 541 and 684 for rotordynamic analysis and shop testing
- Difference between rigid rotor and flexible rotor
- Lateral critical speed analysis, unbalanced response, bearing span, core stiffness
- Finite Element Analysis (FEA) for structural analysis of frame and bearing housings
- Shop mechanical run test
- Impact testing
- Operating deflection shape / modal analysis
- How design and testing steps are implemented throughout the manufacturing and acceptance process

## INTRODUCTION AND LITERATURE SEARCH

There is a large amount of technical literature available on electric motors, rotordynamics, critical speeds, and vibration. For anyone wanting to learn about motors, PCIC / IEEE has a helpful primer series [1-5]. Part 1 presents theory and application information for induction motors typically used at a refinery. Part 2 continues with some discussion on vibration due to rotor eccentricity and lateral critical speeds. Part 3 follows with how to size a motor, discussion on bearings, and what causes motor bars to break. Part 4 covers hydrodynamic journal bearings and how the stiffness and damping properties of the oil film affect the lateral critical speed and unbalanced response of the motor rotor. Finally, Part 5 deals with the topics of torsional vibration, how unbalance and vibration affect motor life, and evaluating motor efficiency.

These and similar papers concentrate more on the motor itself, but not how the driven equipment might affect the motor reliability once installed. A literature search found another helpful paper by Finley and others [6] that covers common sources of motor vibration, flexible or resonant motor base, ways to measure vibration, troubleshooting procedures, a diagnostic chart, and typical vibration alarm levels. Note that these papers do not specifically cover reciprocating compressors and the effect higher shaking forces and alternating torque can have on a motor. A recent GMC paper [7] addressed considerations for motors driving reciprocating compressors, which is out of the scope for this tutorial.

A continued literature search found several excellent papers previously presented at the Texas A&M Turbomachinery and Pump Symposia. Corey [8] presented a review of two-pole induction motor mechanics. Miller [9] presented a tutorial on specifying and selecting large motors. Costello [10] presented a paper on the vibration forces in induction motors. Thornton and Armintor [11] presented the fundamentals of induction motor design and application. Chen and others [12] presented a paper on estimating the “reed” frequency of vertical motors for pump applications. Note that this tutorial is focused on large horizontal induction motors.

The abundance of information begs the question of how to systematically apply some of this knowledge in the design, evaluation, and acceptance of a machine based on vibration criteria. As user and industry specifications become more restrictive it is often assumed that any deviation outside the boundaries of a specification constitutes an unacceptable, problematic, or defective machine. This tutorial attempts to use case studies and other examples to provide some insight regarding the relative importance and consequences of various rotordynamic and structural vibration characteristics. In addition, several definitions are listed to provide the basis for the technical data presented.

## TWO VERSUS FOUR-POLE MOTOR

The speed of an induction motor running across the line will be slightly less than synchronous due to slip. The slip will increase with load. In the US with 60 Hz electrical power, a two-pole (2P) induction motor would operate at slightly less than 3600 RPM, a four-pole (4P) induction motor slightly less than 1800 RPM, a six-pole induction motor slightly less than 1200 RPM, and so on.

For a two-pole motor,  $1\times$  mechanical speed will be nearly the  $1\times$  electrical frequency. However, a two-pole motor will also produce excitation at twice supply frequency, which can cause vibration of the stator end windings. The response can be reduced by reducing the magnetic field, increasing the stator stiffness, or isolating the stator from the frame. Therefore, for a large two-pole motor, it is important for all natural frequencies to have sufficient separation margins from the  $2\times$  electrical supply frequency. Depending on how the stator is supported in the casing, this could also lead to excessive casing / housing vibration. A four-pole motor, on the other hand, will tend to have lower amplitude excitation because the magnetic forces are distributed more uniformly. The four-pole motor could still vibrate at  $1\times$  mechanical speed (slightly less than  $1/2\times$  electrical frequency depending on slip).

A two-pole 60 Hz machine has magnetic forces which tend to deform the stator into an elliptical shape that is rotating at 3600 RPM. On a four-pole 60 Hz machine, the magnetic forces try to deform the stator into a square shape that is rotating at 1800 RPM. It is easier for the  $2\times$  line frequency magnetic forces to deform the stator into these shapes as opposed to more complex modes with more nodal points, as would be the case on slower speed machines with more poles. These rotating magnetic forces can manifest as vibration at 120 Hz which can be transmitted to the frame and bearing supports.

Variable frequency drives (VFDs) allow for motor operation through a wide range of speeds or even overspeed. More users are implementing this capability in the design of their system processes for flexibility and/or energy savings. However, this can increase the chance of exciting a mechanical or torsional natural frequency. VFDs can also create forcing functions at electrical harmonics and switching frequencies.

Rama and Griggs [13] presented a paper on high-speed electric drive applications. Gilon and Boutriau [14] shared their experience with high-speed induction motors. These papers show how a two-pole motor can be used with a VFD to operate well above synchronous speed. Use of a VFD makes it possible to eliminate the need for a speed increasing gearbox. Holopainen and others [15] did a comparison of two and four-pole motors when controlled by a VFD. He also points out the difference in how the magnetic forces try to deform the stator. Francesco and others [16] presented a case study showing the importance of structural modal analysis for a two-pole induction motor in liquified natural gas (LNG) service.

The second author of this tutorial worked on several two-pole motors from other manufacturers that experienced vibration issues. Two examples had motors with speed controlled by VFDs that were driving centrifugal compressors. First, a large 2P motor had frame vibration and was found to be sensitive to the mounting feet. Additional tie-down bolts were added. Second, another large 2P motor had elevated axial vibration of the non-drive end bearing housing. A natural frequency was found near 120 Hz that was coincident with twice electrical frequency. The forcing function was low and related to the magnetic field because the vibration amplitude varied with applied voltage (not load). The drive-end (DE) bearing housing, although similar in design, was somewhat supported by the coupling housing and had lower vibration. It was also demonstrated that a simple bolt-on horizontal support could reduce the axial vibration on the NDE bearing housing. These examples show how 2-pole machines could be more susceptible to vibration issues compared with 4-pole machines.

## LATERAL CRITICAL SPEEDS AND NATURAL FREQUENCIES

American Petroleum Institute (API) developed Standard 541 for form-wound squirrel cage induction motors rated 500 HP and larger [17]. There are sections that cover analysis and testing requirements as well as vibration limits. Another document, API 684 is a technical report (not a standard) that provides a rotordynamic tutorial for lateral critical speeds, unbalanced response, stability, torsional vibration, and balancing [18]. API 684 covers a wide range of rotating machinery from motors to centrifugal compressors. There are other freely available resources such as Gunter's Introduction to Rotordynamics [19], and Leader's paper on Understanding Journal Bearings [20] that go into the detail of modeling.

Rotordynamic analyses and reports are required for API machines. Lateral analyses typically include an undamped critical speed map, unbalanced response, and possibly a stability analysis if operating at higher speeds. The journal bearings need to be modeled when performing the unbalanced response and stability analyses. Proper bearing and coupling selections should be verified as their properties can affect the calculated results and may need to be adjusted accordingly. A steady-state torsional analysis of the entire train (not just the motor) should also be performed. In some cases, a time-transient torsional analysis may be requested. These reports should include the model, methods used, predicted results with plots, clear conclusions and recommendations.

It is essential that resonant frequencies reside outside of the operating speed range, be well-damped, or not significantly excited in order to not generate harmful levels of vibration. Lateral critical speeds refer to the rotor design but can be influenced by the support structure and/or foundation. Other natural frequencies need to be considered such as with the motor frame and bearing housings. The following definitions are provided.

Amplification factor (AF) is a measure of damping. A higher value of AF indicates increased sensitivity to unbalance when operating near a lateral critical speed (lower damping). API 684 provides the following equation

$$AF = \frac{N_{c1}}{N_2 - N_1} \quad (1)$$

where:

$N_{c1}$  = Rotor first critical, center frequency, cycles per minute (CPM)

$N_1$  = Initial (lesser) speed at  $0.707 \times$  peak amplitude (critical)

$N_2$  = Final (greater) speed at  $0.707 \times$  peak amplitude (critical)

Rotor critical speed is defined as the running speed of a rotor that corresponds to one of its lateral natural frequencies. The critical speed is characterized by the frequency of the peak vibration response determined from the Bode plot, resulting from an unbalanced response analysis and shop test data. At resonance, the Bode plot will also show a shift in phase angle. The sharpness of the amplitude peak depends on the damping as already discussed.

Separation margin (SM) is the difference between the operating speed and a resonance. A minimum SM of 15% is required by API 541 for non-critically damped ( $AF > 2.5$ ) rotor system resonance. However, other specifications (such as for municipalities) may require a 10%, 20%, or larger SM.

*Lateral natural frequencies, which can lead to resonance amplification of vibration amplitudes, shall be removed from the operating speed frequency and other significant exciting frequencies by at least 15%. Machines intended for continuous operation on adjustable speed drives shall meet this requirement over the specified speed range. If it is not practical to avoid lateral natural frequencies by at least 15% in an ASD application, a well damped resonance may be permitted with purchaser approval.*

Owen [21] discusses flexible shaft versus rigid shaft electric machines. A ‘rigid shaft’ design is when a machine operates below the first lateral critical speed by at least a 15% margin. Whereas a ‘flexible shaft’ design is when the operating speed is above the first lateral critical speed. In this case, the rotor will pass through at least one critical speed as it accelerates to full speed. More recent terminology refers to lateral critical speeds that are below running speed as sub-critical. Whereas lateral critical speeds above running speed are now called super-critical.

A ‘critically damped’ rotor design may operate on a natural frequency if the response demonstrates an AF of less than 2.5. With this level of damping, API no longer considers this to be a critical speed of concern, therefore no SM is required for these modes. Therefore, from a practical standpoint, the design would be somewhat like the rigid shaft in that no restrictions are imposed on the operating speed.

Leader [22] refers to the term ‘semi-rigid’ in his paper. The term ‘semi-rigid’ has also been used because in some cases an overspeed coast down plot may show a non-critically damped peak above the operating speed and a critically damped peak within the operating speed. Although useful to differentiate between different design approaches at the design phase, from a user standpoint the labels ‘critically damped’ or ‘semi-rigid’ need not be a part of the nomenclature since they may cause confusion or imply an operational limitation.

Frame Structural Resonances. API 541 states that the frame of the completely assembled machine on its permanent foundation, with the rotor installed and rotating on its oil film, shall be free from structural resonance within  $\pm 15\%$  of one and two times the electric line frequency, between 40% and 60% of running speed, and  $\pm 15\%$  of one and two times running speed. For example, a two-pole motor operating at 3569 RPM with 60 Hz line frequency should therefore not have any resonances in the following frequency ranges: 24 - 36 Hz, 51 - 69 Hz, and 102 - 138 Hz.

Frame Structural Resonance Limits. API 541 states that the magnitude of the unfiltered horizontal vibration of any loaded structural member of the frame along the axis of the shaft centerline shall not exceed two times the limit given below when operating at no-load, full voltage, and rated frequency. Measurements shall be taken on the outside of the machine at the loaded structural member of the frame. A loaded structural member of the frame is defined as one of the steel plates or structural sections that support the stator core in the case of box frames. For other designs, measurement points shall be agreed between the vendor and purchaser prior to the purchase order.

Limit =  $0.1 \times N/1000$  where N is rated speed (RPM) and the units are inches/sec 0-p  
For the two-pole motor example, this would be 0.36 ips 0-p.

Bearing Housing Natural Frequency. API 541 states that, when specified, bearing housings or end bracket supports shall be checked for resonance on one fully assembled machine of each group of identical machines. This can be done using impact tests or shaker tests. The resulting response shall be plotted for a frequency range of 0% to 400% of line frequency. To eliminate the interaction between the bearing housings the rotor shall be turned at a slow roll (200 to 300 RPM). The response plots shall be made on each bearing housing in the horizontal, vertical, and axial directions. The application of the excitation force shall be made in these same directions. No significant resonance shall occur within  $\pm 15\%$  of one and two times running speed,  $\pm 15\%$  of one and two times line frequency, or between 40% and 60% of running speed. A significant resonance is defined as a peak that lies within 6 dB in amplitude (displacement) of the fundamental bearing housing resonance in the direction being tested. Percentages are based upon one times running speed and electric line frequency.

## ROTOR DYNAMIC DESIGN OF 4500 HP TWO-POLE MOTOR

A two-pole induction motor, rated for 4500 HP, was designed to operate over a wide speed range to be free of rotor critical speeds. It will be referred to as serial number 4500HP2P. Table 1 summarized the customer requirements.

Table 1. Customer Requirements for 4500HP2P Motor

Voltage	4000
Poles	2
Frame	7111
Rated Power	4500 HP
Bearings	Sleeve (Flood lubrication with oil ring as backup)
Operating Speed	40% below rated speed to 10% above rated speed (2160 – 3960 RPM)
Critical Speed	Min. 15% above maximum operating speed. ( $1.15 \times 3960 \text{ RPM} = 4554 \text{ RPM}$ )

The design needed to achieve a first critical speed of at least 4554 RPM or be critically damped ( $AF < 2.5$ ) if near the operating speed range. These same criteria were also applied to the second critical speed. Therefore, a rigid or critically damped shaft rotor was required. The basic overall geometry used is depicted in Figure 1.

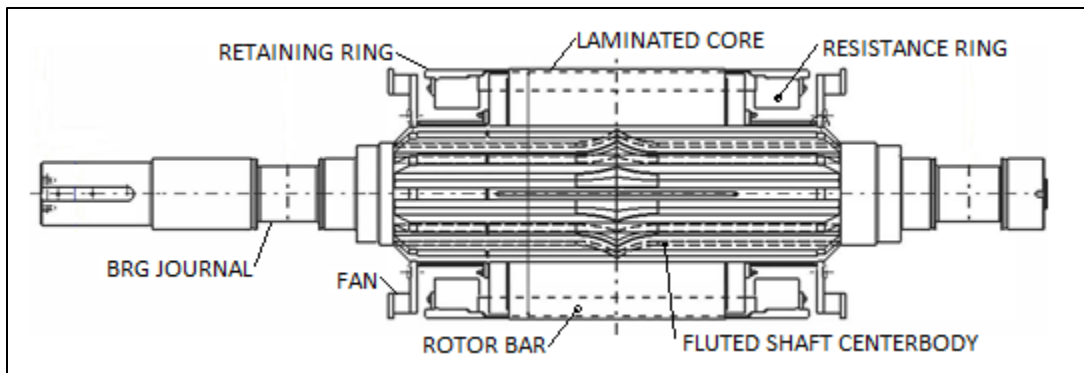


Figure 1. Rotor Geometry

### Rotordynamic Analysis

A rotor model was created as shown in Figure 2. It includes unbalance for the coupling and at each end of the core (indicated by triangles). The mass of the motor core was distributed along the motor shaft (shown as circles). Note that modeling an induction motor core as only a single mass is not recommended and could lead to inaccurate analysis results. Bearing oil film and bearing housings are also included in the model (labeled as stations 25 and 26).

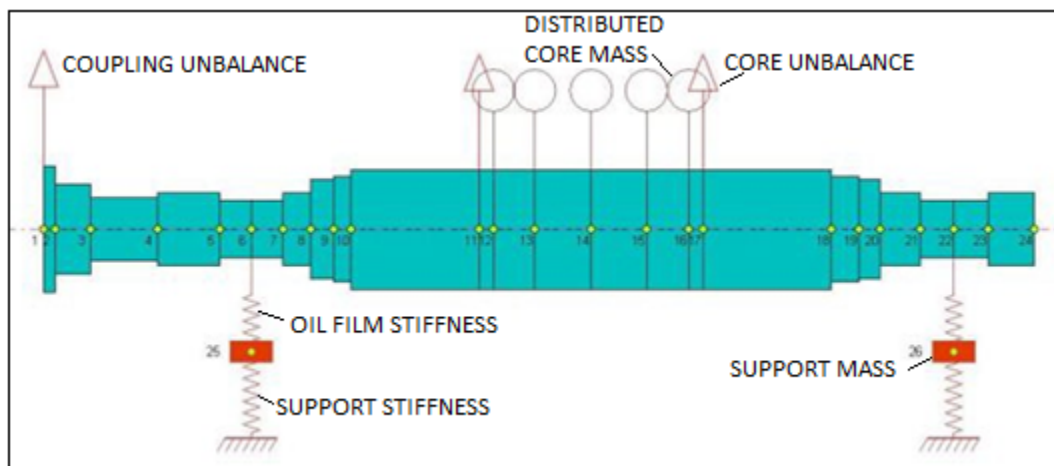


Figure 2. Rotor Model



There are many parameters that affect the rotordynamics of a motor. In general, the following parameters can have a significant influence on the critical speed performance:

- Bearing span
- Motor core length, weight, and shaft diameter
- Bearing characteristics (which are primarily a function of bearing type, housing stiffness and oil film properties)
- Motor core stiffening (spider/fluted shaft, interference fit between core and shaft, and rotor core stacking pressure)
- Structural support stiffness and foundation

Although each case is unique, the most important component of a system can usually be detected by review of the potential (i.e., strain) energy distribution [23]. The potential energy plot shows the relative energy contribution of the bearings, shaft, and supports to the overall rotordynamic system. The energy contributions and plot are generated by the software and is shown in Figure 3. In this case the bearings are the highest contributors, which indicates that a change to the bearing stiffness parameters would have the most influence on the undamped critical speed location.

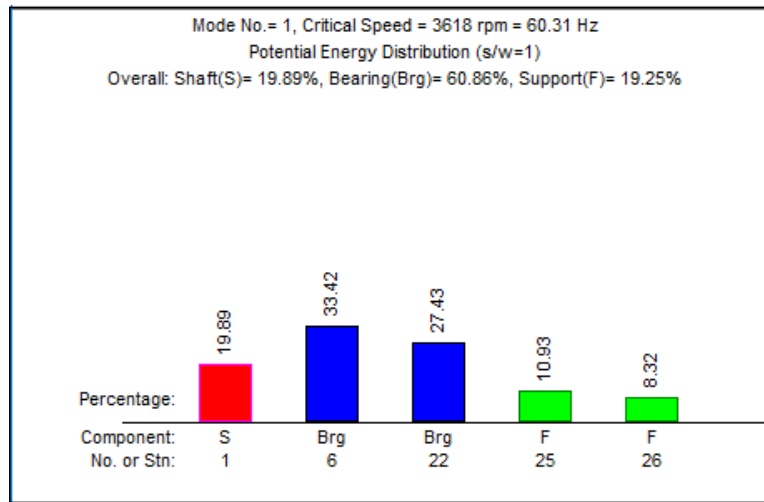


Figure 3. Energy Distribution

### Effect of Bearing Span on First Critical Speed

The bearing span is the distance between the bearing centerlines. A longer span will lower the stiffness and natural frequency. The following equation [24] can be used to estimate the natural frequency of a uniform round shaft made of carbon steel that is simply supported at each end

$$f_1 \approx 79200 \frac{D}{L^2} \quad (2)$$

where  $f_1$  is the first natural frequency of the beam in Hz,  $D$  is the diameter and  $L$  is the span in inches. For example, a round steel shaft with a 4" diameter and length of 60" would have a natural frequency of approximately 88 Hz or 5280 CPM.

The Jeffcott rotor [25] is a simplified model where the mass is concentrated at the midspan. However, for the first mode, the *modal* mass of the shaft will be half of the *total* mass of the shaft. Therefore, the natural frequency can be calculated from

$$f_r = 3.13 \sqrt{\frac{K_s}{W_m}} \quad (3)$$

where  $f_r$  is the rigid bearing critical in Hz,  $K_s$  is the shaft stiffness (lb/in), and  $W_m$  is the modal weight, concentrated weight at the midspan plus half of the shaft (lb). The following equation from reference [24] can be used to estimate the lateral stiffness of a round steel shaft

$$K_s = (70.7 \times 10^6) \frac{D^4}{L^3} \quad (4)$$

Using Equation 4, a round steel shaft with a diameter (D) of 4" and length (L) of 60" has a calculated lateral stiffness of 83,800 lb/in. The shaft weight is 213 lbs. If a concentrated weight of 300 lbs is attached at the midspan of the shaft, then the modal weight would be  $213/2 + 300 = 406.5$  lbs. Using Equation 3, the natural frequency would be approximately 45 Hz or 2700 CPM.

As shown, the natural frequency can be raised by an increase in shaft stiffness or lowered with additional weight. Reducing the bearing span will typically increase the natural frequency; however, there are several factors to be considered before adjusting the bearing span. For a 2P machine, length over end turns (LOET) is usually very long due to wide coil span, and insulation clearance between the coil and any metallic component as well as required air flow area dictate the minimum allowable length of the machine. Core offset can also be used to minimize the additional length required for the end turn connections. Lastly, shaft mounted axial fans and internal air baffles can also affect the bearing span.

### ***Core Length, Weight, Shaft Diameter, and Core-to-Shaft Fit***

In general, using the shortest bearing span possible is best when attempting to maximize rotor stiffness. For a given rating the stator diameter and core length will dictate the frame size of the machine. One method to reduce the core length and maintain the same performance would be to increase the rotor and stator diameter proportionally. The core diameter squared times the core length ( $D^2L$ ) factor can be used to estimate the effect of implementing a different diameter or length. For example, for a given power rating:  $D_1^2L_1 \approx D_2^2L_2$ . However, it must be kept in mind that an increase in diameter may lead to a much heavier rotor which can nullify any positive effects of a shorter core and bearing span. Moreover, a diameter increase may require an increase in shaft height, which may not be possible, especially when designing machines to fit in existing installations.

As rotor diameter increases, not only does the required shaft elevation (and frame size) increase, so does the hoop stress in the laminations. Machines with a shaft centerline height of over 630 mm ( $\approx 25$  inches) may use rotors with outer diameters that result in unacceptably high lamination stress. This can be mitigated by using higher strength material and/or laminations that have no axial ventilation passages. Ventilation openings in the laminations reduce the cross-sectional area and can also introduce stress risers. A lamination without ventilation openings is more robust, but also requires an alternate method of cooling the rotor. In most cases this is accomplished by the use of a spider or fluted shaft (as shown in the example rotor in Figure 1) to allow air flow between the shaft OD and lamination ID. With proper design of rotor bore and shaft arm geometry high lateral shaft stiffness can be maintained while also providing sufficient ventilation. If stiffness can be increased while minimizing the mass, the natural frequency will be elevated. The quantity, width, and height of shaft arms have a direct relation to stiffness. The main restrictions are the physical limits and ventilation area requirements.

Use of a fluted shaft design requires calculation of an equivalent lateral stiffness and mass for the portion of the shaft where the arms are located. An increase in stacking pressure and interference fit between shaft and core will also increase the overall stiffness. It is difficult to quantify the effect of these parameters without experiment. Note that the effect of motor core stiffness is discussed in more detail in a separate section of this tutorial.

The 7111 frame 2P motor in this case study used the motor manufacturer's standard 12-inch diameter fluted shaft with the standard diametrical interference of 0.012 - 0.014 inch. Since the core length was only 19 inches and the shaft was fluted, the contribution of the stiffening effect of the shrink fit was not considered to be conservative. Past experience indicates that the stiffening effect of the interference fit is lower on fluted shaft machines, and especially those with short cores. A general rule of thumb is to assume an increase in the shaft stiffness diameter of 10% or less when analyzing shafts with arms, unless heavy interference and core stacking pressures are used.

### ***Sleeve Bearing Performance and Stability***

The sleeve bearing performance has a significant effect on the critical speed by altering the rotor support stiffness and damping due to the bearing housing and oil film properties. The motor manufacturer currently uses a commercially available program to calculate bearing performance parameters. The bearing manufacturer may also be able to provide the stiffness and damping coefficients.

The bearing size was chosen based on the minimum diameter required to transmit the torque and that would also obtain the highest stiffness and damping of the oil film using a standard catalog sleeve bearing with a loose oil ring. Larger journals are generally better from a stiffness and damping standpoint, but larger diameters also reduce specific pressure. Low specific pressures generally result in lower oil film stiffness and can make the design more susceptible to oil film instabilities, such as oil whirl, especially if the pressure is below about 80 psi. Specific pressure is the journal load divided by the journal projected area. This is also commonly referred to as "unit load."

Finally, a large journal diameter also has a higher peripheral velocity which can result in oil ring instability. Oil rings are used in most plain journal bearings to pick up oil from the bearing sump and lubricate the journal as the ring rotates at a fraction of the journal speed. They are technically not needed on pressure lubricated bearings but are normally left in place as a backup in the event of a lube system failure to allow shutdown without overheating or damage. However, for large journals at high speeds the ring can become unstable, and this must be a consideration. The bearing supplier normally has published limits for maximum allowable journal peripheral velocity when a bearing with an oil ring is used.

The bearings selected use oil rings but still require an external source of flood lubrication to maintain a reasonable oil film temperature (typically  $\leq 93$  C per API). The oil film stiffness and damping coefficients were calculated for many discrete speeds throughout the operational speed range for a selected oil viscosity and radial clearance based on the bearing manufacturer's recommendations for oil supply temperature and flow rate. A journal diameter was selected that could not only transmit the required torque but would also provide the optimum radial clearance to obtain the highest level of oil film stiffness and damping.

Larger journal diameters are desirable from a stiffness and torque transmission standpoint but have the undesirable effect of reducing the bearing specific pressure as mentioned above. A lightly loaded, fixed geometry bearing can contribute to oil whirl and whip instabilities due to small journal eccentricity and large attitude angle. Eccentricity is the relation of the shaft centerline location with respect to bearing centerline. The lower the eccentricity the more the shaft centerline is approaching the bearing centerline, which is a position of reduced stability. The eccentricity ratio is  $e/c$  where  $e$  is the distance between the centers of the shaft and bearing, and  $c$  is the radial clearance (value of eccentricity ratio ranges from 0 to 1). Zero eccentricity would mean the shaft is centered within the bearing.

Attitude angle is a characteristic of horizontal sleeve bearings and is obtained by drawing a line from the geometric center of the bearing through the rotational center of the journal, and then measuring the included angle between the negative "Y" axis and this line. The greater the load the more closely the journal rotational center is lined up with the negative "Y" axis. As the load decreases the attitude angle increases as well as susceptibility to instability. This angle is generally one of the outputs of the bearing design software.

It is also generally desirable to decrease radial bearing clearance to increase the stiffness and damping of the oil film, but this could have the undesirable effect of reducing eccentricity and increasing attitude angle. Fortunately, when the shaft is designed to have the first lateral critical speed well above running speed (super-critical), the system should be less sensitive to low eccentricities and large journal attitude angles. This is typically the case when the shaft contributes 30% or less to the overall potential energy of the system, as previously shown in Figure 3.

The final design in this case study resulted in a specific pressure of 88 psi, an eccentricity ratio of 0.28, and an attitude angle of  $62^\circ$ , but with no indication of operational instability for more than ten years of operation to date. Conversely, on flexible rotor designs a general guideline is to try to achieve a calculated journal eccentricity ratio of at least 0.5 and an attitude angle of less than  $40^\circ$  to avoid sub-synchronous instabilities. For a stable system, the predicted logarithmic decrement (log dec) of sub-critical frequencies should theoretically be positive, but in practice should be at least +0.1.

API 684 states that the key to stability robustness is the optimization of bearing characteristics relative to the shaft stiffness. One guideline for a stable rotor [24] is for the stiffness ratio ( $2 \times K_b / K_s$ ) to be less than two, where  $K_b$  is the bearing stiffness and  $K_s$  is the shaft stiffness. If the bearing stiffness is much higher than the shaft stiffness, then this becomes similar to the Jeffcott rotor already discussed. Flexing will occur in the shaft as opposed to motion across the bearing oil film.

The bottom line is that bearing type, size, clearance, and oil viscosity must all be considered when calculating the overall performance as a function of speed and load. Other types of bearings, such as four-lobe or tilting pad may be needed in some cases. With less cross-coupling of the oil film properties these bearings are inherently more stable and normally provide more uniform performance in the horizontal and vertical directions. This can be useful to help shift non-critically damped horizontal peaks further above running speed to increase separation margin.



### Support Stiffness

The combined stiffness from the rotor to the ground can affect the lateral critical speeds. It is therefore important that the motor be mounted on a stiff foundation and not a flexible base, which could have its own resonances. When considering support stiffness, the energy distribution plot from the rotordynamic software (Figure 3) becomes very useful. If this plot indicates support stiffness to be a major factor, then the components included must be considered individually. Not much can usually be done about the bearing housings or foundation, which leaves only the bearing brackets and motor frame as potential candidates for changes. Fabricated machines with thick steel bearing supports and sleeve bearings generally result in combined structural support stiffness greater than  $3 \times 10^6$  lb/in for both the horizontal and vertical directions when mounted on a massive foundation. This can be verified by finite element analysis as well as by impact or shaker testing. It is usually difficult to make structural changes that have a significant effect on this parameter. For this case study, special bearing brackets were designed to maximize both radial and axial stiffness. The radial (i.e., lateral) support stiffness value was estimated to be  $3.5 \times 10^6$  lb/in for the horizontal and vertical directions.

### Lubrication Viscosity

More viscous oil could provide more damping. However, the effective damping could be less since the stiffness could also be higher. Therefore, the designer needs to consider the impact of the stiffness and damping coefficients. To determine the effect on a critical speed, a full lateral analysis is still required. As mentioned before, bearings behave differently under different conditions such as speed, temperature, clearance, geometry, etc.

### Analytical Results

The initial analysis showed that the machine physical size limitations, expanded speed range, plus the 15% separation margin were, when all taken together, too restrictive to allow a design in which there would be no dependence on critical damping at certain speeds. Therefore, the end user agreed on a critically damped design. This required additional analyses to ensure the performance would be achieved. Rotordynamic analyses included unbalanced response calculations based on both the minimum and maximum possible bearing clearance. Table 2 shows the final motor parameters.

Table 2. Final Motor Parameters

Bearing Type (DE and NDE)	14-125 and 14-125 Insulated
Bearing Journal Diameter	4.9150 / 4.9155 in
Diametrical Bearing Clearance (~15% reduction)	0.005 / 0.008 in
Bearing Span	59.7 in
Core Length	19 in
Oil Lubrication Grade	ISO-VG 32
Number of Arms	12
Arm Width	1.5 in
Arm Height	1.5 in
Shaft Base Diameter through Core Section	9 in
Equivalent Round Shaft Diameter at Fluted Section*	10.39 in

\*Equivalent round diameters of fluted shafts can be determined by using the area moment of inertia of the cross section as obtained by calculation, CAD, or FEA, and calculating a round diameter to provide that same inertia.

Table 3 summarizes the final analysis results. It is important to consider the full range of bearing clearance. For the minimum and maximum bearing clearances, the critical speeds in the vertical direction were calculated to be more than 15% above the maximum operating speed and therefore meet the required SM. However, the critical speeds in the horizontal direction were predicted within the operating range of 2160 to 3960 RPM. Since the predicted AFs were below 2.5, the horizontal critical speeds are considered to be well damped. Therefore, a SM is not required since these will not impact operation.

Table 3. Final Analysis Results

	Min. Clr.	Max. Clr.
Critical Speed (Horizontal)	4200 - 4250 RPM	3400 - 3450 RPM
AF (Horizontal)	n/a	1.4 - 1.5
Critical Speed (Vertical)	5450 RPM	5400 RPM
AF (Vertical)	6.7	4.4 - 9.5

Unbalanced response plots are shown in Figures 4 and 5.

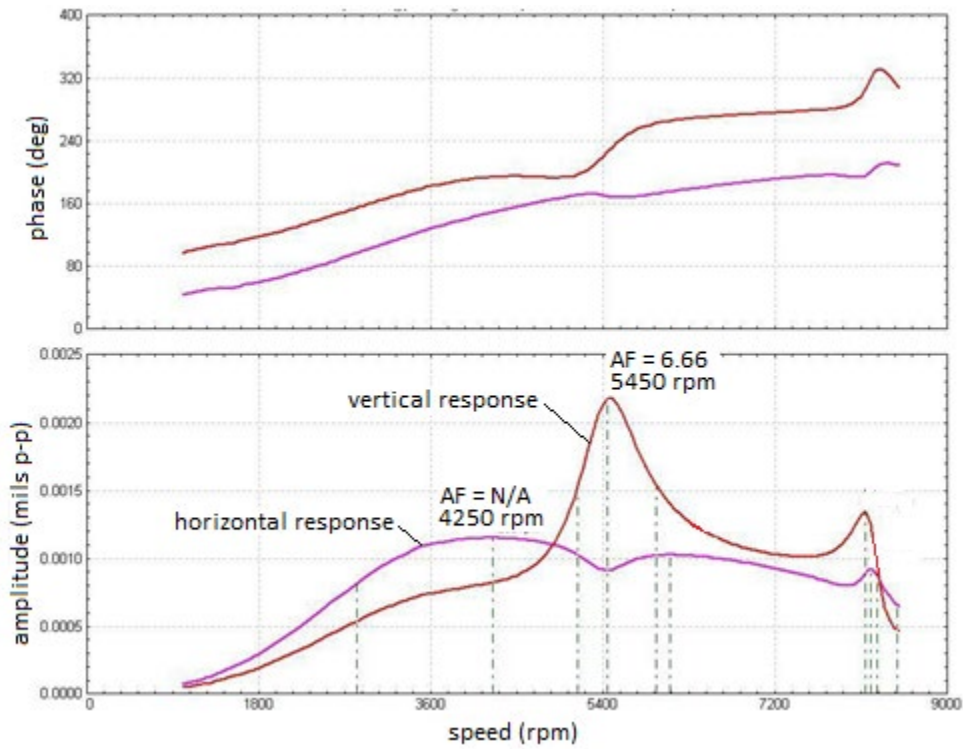


Figure 4. Bode Plot in X and Y Direction at DE Journal (4W/N Unbalance & Minimum Clearance)

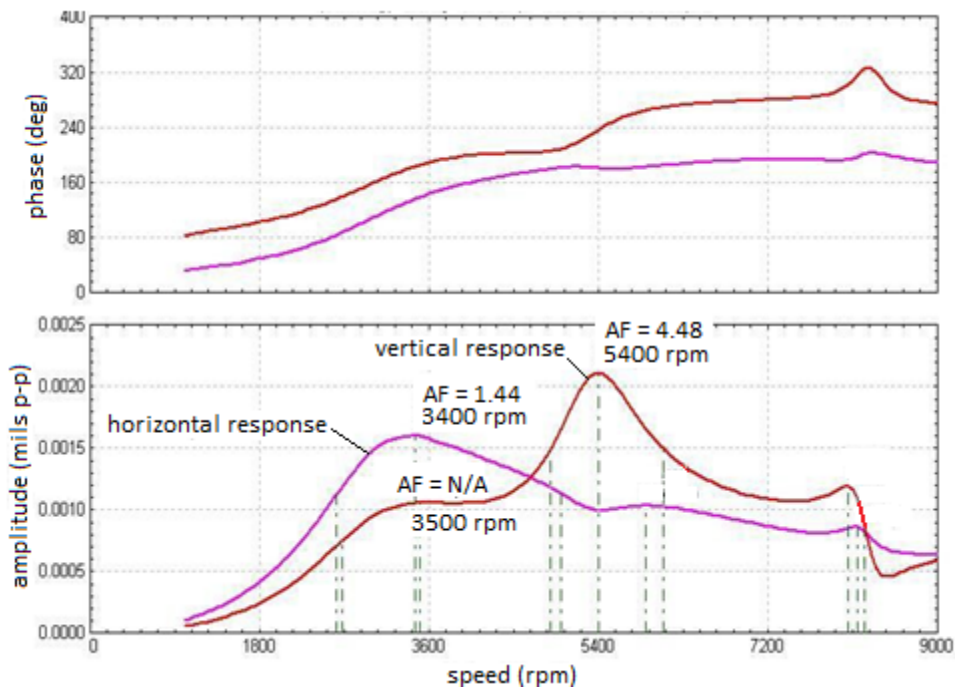


Figure 5. Bode Plot in X and Y Direction at DE Journal (4W/N Unbalance & Maximum Clearance)

### Test Results

Figures 6 and 7 show coast down data from an unbalanced response test. Note the data were collected using an ADRE 208P, and when amplitudes are low compared to the full-scale range, the system was not able to determine the phase angle.

Although the plot cuts off at slightly above 4300 RPM, the peak was above this speed, which means the machine will not operate within any critical speed region. The bode plots do show a very slight increase between 3200 and 3600 RPM, but is of very low magnitude, nearly zero phase change, and highly damped as predicted. When considering the overall speed range scale of the predicted and test plots, comparison of the data shows a very reasonable correlation.

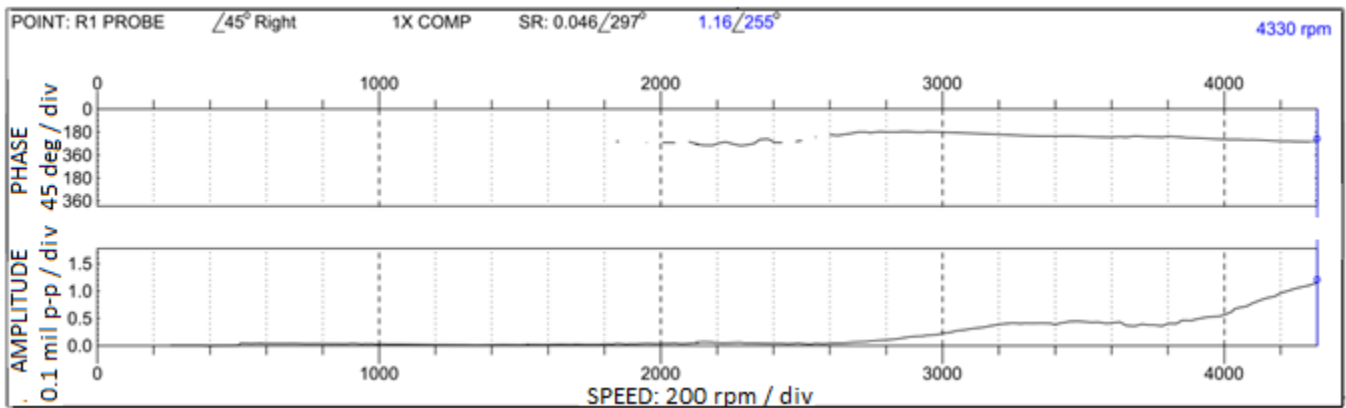


Figure 6. Unbalanced Response Coast Down Plot in X Direction at DE Journal

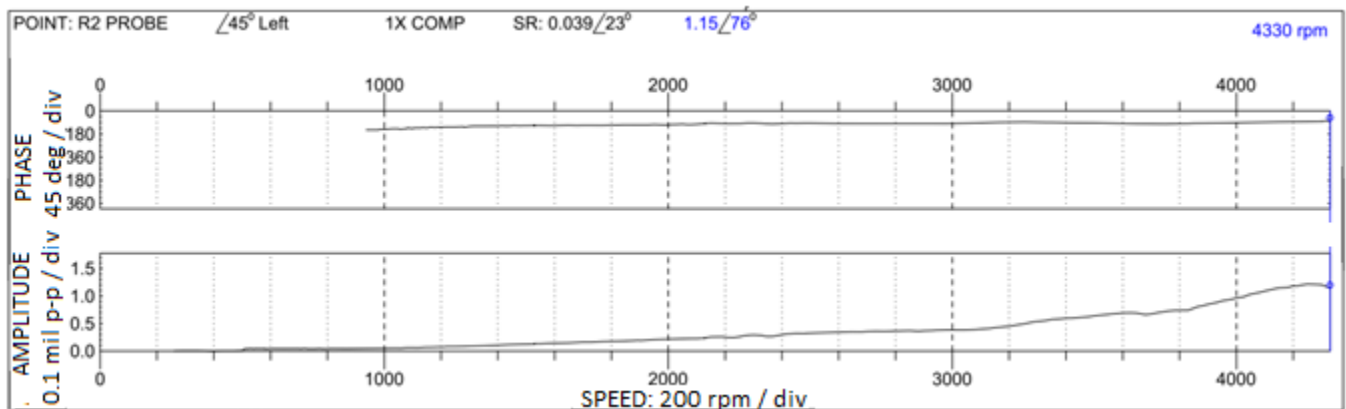


Figure 7. Unbalanced Response Coast Down Plot in Y Direction at DE Journal

### Summary

This example shows how a critically damped design was accomplished for this frame size. Many parameters were considered as previously discussed. In the end it is believed the optimal design was chosen. The test results demonstrate that incorporation of known design features along with robust analyses make it possible to design a reliable, well-damped rotor which can operate over a wide speed range.

## EFFECT OF MOTOR CORE STIFFNESS

This section provides additional discussion on the effect of motor core stiffness on lateral critical speeds and provides some suggestions for how to determine an equivalent value. The effective core stiffness can be influenced by operating speeds and temperatures as shown in the following example.

### Example 1

A vibration issue stemming from a reduction in critical speed from the cold to hot condition provides some sense as to the significance of the interference fit. As an example, a 4P 5616 special frame was designed to replace some very old motors. They were the standard round shaft design but used a non-standard 48-inch core length and increased bearing span. This required that the default standard design limit of 40 inches for this size of machine be over-ridden.

There were two identical units (01 and 02) except for what was found to be a different level of interference between the shaft and core due to manufacturing tolerances. The *calculated* critical speed, based on an assumed increase of shaft stiffness by 15% to account for the shrink fit effect, was 2200 RPM, but dropped to 1900 RPM when no additional core stiffening was included in the model. The tested values in the cold and hot conditions are shown in Table 4. Note that the first critical speeds should be at least 2070 RPM to meet the minimum required SM of 15% from the operating speed of  $\approx 1800$  RPM.

Table 4. Tested Values

***TESTED 1ST CRITICAL***				
	COLD	AF	HOT	AF
52504P01	2140 RPM		2110 RPM	
52504P02	2034 RPM		1920 RPM	5

Based on the QA records, Unit 1 had a diametrical interference of 0.007 inch and Unit 2 had an interference fit of 0.005 inch. Therefore, Unit 2 had less shaft/core interference. Both values were within the required tolerance. Unit 1 was shipped and the shaft vibration was within tolerance in the uncoupled condition. However, after sitting idle at the customer site for several months, the un-coupled shaft vibration increased to near alarm levels during a test run.

The motor was returned and both units were rebuilt with a new core using laminations with a larger bore, which allowed a larger diameter shaft from the next higher frame size. By doing so the calculated critical increased to 2200 RPM based only on the increase in shaft stiffness due to the larger diameter. No additional core stiffening effect due to shrink fit was assumed. The new interference value used was 0.008 to 0.010 inch diametrical. Overspeed coast down data for the new design was truncated at 2150 RPM, but slope of the curves indicated the critical speed to be something greater than 2150 RPM in the no-load condition. No coast down data were obtained at the rated temperature. Both units were tested, shipped, and put into operation without incident.

### Example 2

In another, separate example, the second author conducted measurements on a rotor from another manufacturer. The rotor was first suspended from a crane and impact tested. The first two measured natural frequencies should correspond to the third and fourth modes on the left side of a critical speed map (no stiffness). Next, the rotor was placed on “knife edges” positioned to match the bearing centerlines and impacted again. The measured natural frequency should ideally correspond to the first mode on the right side of the critical speed map (rigid stiffness). Note it could be tricky to match all of the modes.

The rotor model was adjusted by increasing the Young’s Modulus of the shaft section through the core until the predicted natural frequencies generally agreed the impact test results. From this exercise, it was estimated to use an equivalent value of  $E=100 \times 10^6$  psi (instead of  $30 \times 10^6$  psi normally used for steel) for the shaft section under the core.

### Summary

There are several assumptions used in industry to account for the increased lateral stiffness through the motor core. When analyzing shafts with arms, unless heavy interference and core stacking pressures are used, an increase in the equivalent shaft diameter might be 10% or less. Other assumptions as discussed in this section include a 15% increase in stiffness or using an effective Young’s modulus of  $100 \times 10^6$  psi through the core section, depending on the motor construction. When possible, it is best to obtain experimental data because it is difficult to accurately model and calculate the effective core stiffness due to the spider bars, stacked lamination, effect of shrink fit and tensioning, etc.

## VIBRATION RESPONSE AND STRUCTURAL ANALYSIS

During testing, the vibration as measured on the bearing housing of 4500HP2P was slightly higher than expected in the axial direction. The axial vibration spectrum demonstrated the typical 1× and 2×, and some 3× line frequency components as shown in Figure 8. For 3600 RPM machines the API bearing housing vibration limit is 0.1 in/sec 0-p overall. During the initial test, the axial vibration reading periodically approached and slightly exceeded this limit at certain speeds within the speed range.

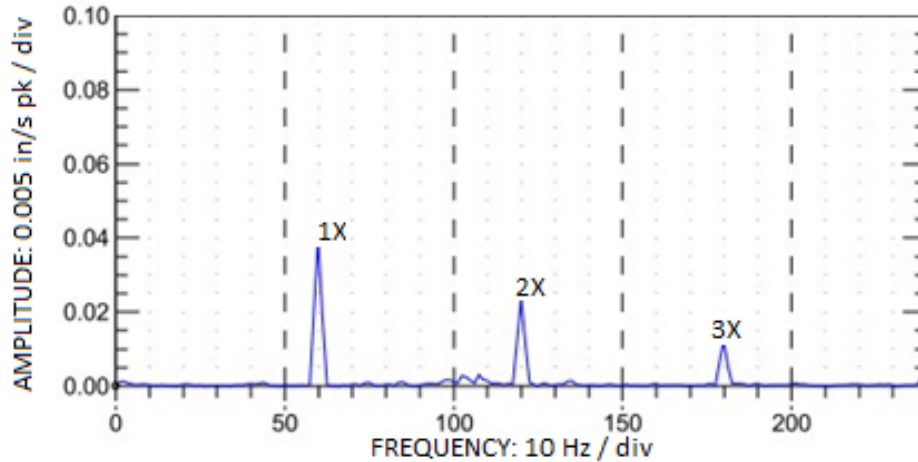


Figure 8. Original Axial Vibration Spectrum, DE Bearing Housing

Bump testing conducted on the bearing bracket while mounted on the frame revealed structural peaks near 100 and 125 Hz in the axial direction. Rather than focus on those frequencies where the axial vibration was the highest, the initial effort was directed toward addressing any structural resonances near 120 Hz. The logic was to focus first on achieving compliance with the API resonance restrictions, and then to address any additional remaining non-compliances as needed.

A simple bump test can identify natural frequencies but would not tell anything about the mode shape unless combined with modal or operational deflection shape analysis. Modal analysis should normally be part of the bump testing process. However, at the time of this study the bump testing was initially used only to detect natural frequencies, and finite element analysis (FEA) was used to in an attempt predict the mode shapes at those frequencies.

In theory, if the FE model predicts a mode at nearly the same frequency as the bump test peak there can be a high degree of confidence in the model accuracy as well. Even though FEA software has improved greatly, modal analysis based only on the FE model can still be very challenging due to its dependence on boundary conditions and various assumptions. A major factor affecting the accuracy of FEA results is the boundary conditions. These include the bracket-to-frame interface, motor frame feet to foundation, stator mass and stiffness, and external supports or loads, if any. Knowledge and experience are essential for applying appropriate boundary conditions to the FE model.

### *Analyses*

For a machine that will be operated over a wide speed range it would be very difficult, if not impossible, to avoid operation on or near a structural resonance at some point within the operating band. Therefore, the goal was to achieve a design that would first comply with the resonance restrictions as defined by API at the rated operating condition, and then address any non-compliant vibration conditions at other speeds if needed. It was hoped that if the 125 Hz axial structural peak could be moved further away from an excitation frequency, then the 120 Hz component, and consequently the overall vibration would remain within the required 0.10 ips peak limit throughout the speed range. Three different bracket configurations were fabricated. Analyses were performed for each design to compare with the test results. The three main stages of analysis were as follows:

- Bracket only to simulate a free-free condition.
- Bracket with boundary conditions to simulate the bump test result.
- Different bearing bracket/frame designs.



### Using Bracket Only to Simulate Free-Free Condition

To help determine the accuracy of FEA prediction, a bump test in the free-free condition was performed. Bump testing was performed while only the original bracket (without bearing housing) was suspended by a hoist. In FEA the same condition can be simulated by using a weak spring as a support.

The comparison in Table 5 shows a reasonable correlation between test and analysis results. Since the bracket was not mounted on the motor frame it was not expected to show an as-built resonance, but only to verify accuracy of the FE bracket model. Note that no peak was detected near 125 Hz while in this condition.

Table 5. FEA Natural Frequencies for Bracket in Free-free Condition

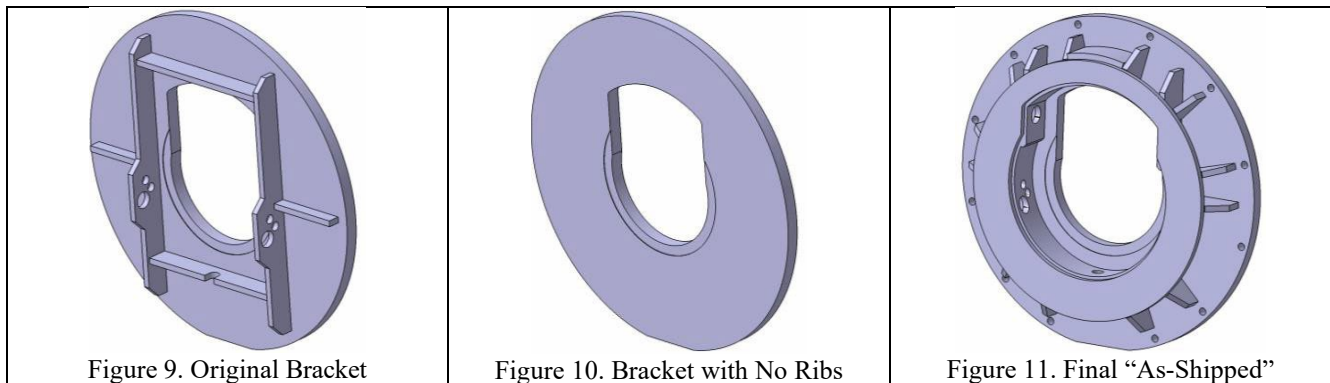
Mode	FEA Prediction (Hz)	Test Frequency (Hz)
1	136	130
2	197	190
3	344	310
4	372	380

### Adding Boundary Conditions

The initial analysis done with the free-free bearing bracket did not provide useful results other than to verify the FE model of the bracket alone. The next step was an attempt to apply more realistic boundary conditions. For each bracket design, bump testing was performed with the brackets bolted to the frame so that the results were actually the response of the whole system. Likewise, all subsequent FE studies included a simplified model of frame, stator, rotor and bearing brackets.

### Different Bearing Bracket/Frame Designs

Frequency Correlation – throughout this process, three different brackets were made and tested: original bracket, bracket with no ribs (stiffeners), and the final “as-shipped” bracket as shown in Figures 9, 10, and 11, respectively.



### Original Bracket

After re-installing the original brackets (Figure 9) as well as modeling the entire system, another axial bump test confirmed the existence of the original peaks near 100 and 125 Hz as previously mentioned. These were compared to the FE model predictions of a 96 Hz axial mode and a 131 Hz side-to-side frame mode. It was hoped that the FE model would show a mode near 125 Hz which would correspond with the bump test result, and that a better understanding of the mode shape could then be used to determine what structural changes would have the most effect on axial stiffness. Since the FE predictions did not seem to show any axial modes corresponding to axial bump test data, the lack of correlation was attributed to possible error(s) in the boundary conditions, inaccuracies in the frame model, or incorrect assumptions related to the stator core stiffness. In the meantime, while trying to refine the FE model, it was assumed the measured axial peaks must be related to the bearing bracket design even though not reflected in the FEA results. Therefore, several bracket designs were proposed and tested. In addition, the 125 Hz bump test peak was a violation of the bearing housing natural frequency test requirement as per the API definition and was considered a potential contributor to the slightly elevated 120 Hz component of vibration.

### Bracket with No Stiffeners

A first attempt to move the axial bump test structural peak further away from 120 Hz involved removal of the stiffeners (Figure 10) to lower any resonance well below 120 Hz. A subsequent bump test revealed the new axial peaks to be near 102 and 111 Hz, but axial vibration performance did not seem to improve.

### *Final “As-Shipped” Bracket Design*

Initially, the bracket and system deflection shapes were unknown as mentioned. As the testing progressed, however, multiple bump tests were taken at various locations on the machine mounted bracket to obtain both magnitude and phase information. This data began to provide some basic understanding of the bracket mode shape. Knowing the mode shape helped provide information on the optimum location to add supports to increase stiffness. The final, and very robust, design is shown in Figure 11. Although this did not have significant effect on the axial vibration performance, it did show slight improvement, and therefore was chosen as the final configuration. A final axial bump test showed a new overall structural axial peak near 115 Hz, which was higher than the test with “no-stiffener” bracket, but lower than the 125 Hz using the original bracket that had the simple “picture frame” type stiffener arrangement. These results were disappointing since it was believed that the stiffer bracket would serve to increase the axial natural frequency. After all this effort it turned out that the axial peak seen in the original bump testing data had less to do with bracket stiffness and more to do with an overall axial mode of the entire frame structure. Since the new bracket had more mass, the overall axial mode was lowered.

### **Final Design and Test Results**

As a result of the bump testing with the different bracket designs with only limited success, more attention was focused on the frame structure since none of the initial bracket FE studies had indicated a bracket axial mode near 120 Hz. After further refinement of the FE model using improved boundary conditions, better correlation with the FEA was finally achieved by showing an overall frame axial “rocking” mode near 120 Hz, which was reasonably close to the 115 Hz bump test measurement. It was found that a major factor affecting the overall frame/bracket axial mode predicted by the FEA is the assumed boundary conditions of the bolted joints between the bracket and frame structure. Modeling the bolts as beam elements at each discrete bolt location seems to provide the best correlation between analysis and test. With a more refined FE model and a better understanding of the actual mode shape, various frame top plates were investigated to help stiffen the frame axially. The result was to add a 2" × 4" steel axial stiffener from end-to-end underneath the top plate. Figure 12 shows the FE models of the original and final designs.

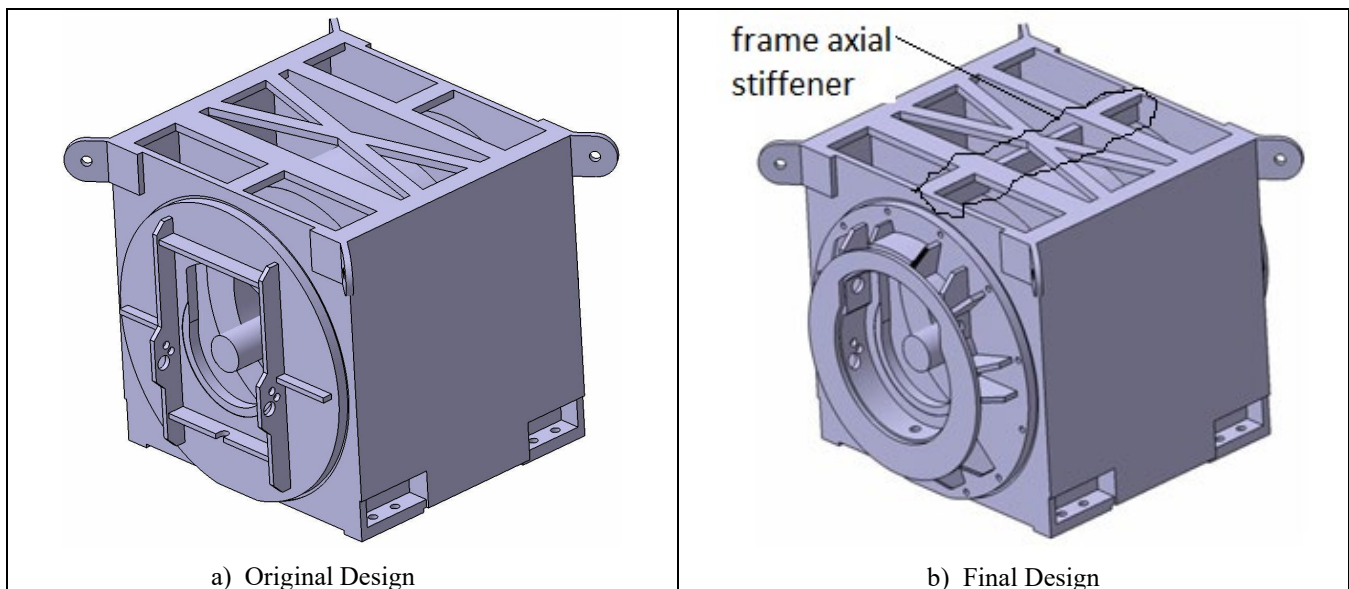


Figure 12. FE Models of Motor Frame and Bearing Brackets

The overall axial vibration level decreased significantly and remained within the limits throughout the speed range and the motor was shipped. Although the required 15% SM between the 115 Hz axial peak shown on the bump test (Figure 13) and the 2× running and line frequencies could not be achieved, all vibration limits were met and maintained throughout the operating speed range. The 2× and 3× components seen in the original running test data spectrum nearly disappeared as shown in Figure 14.

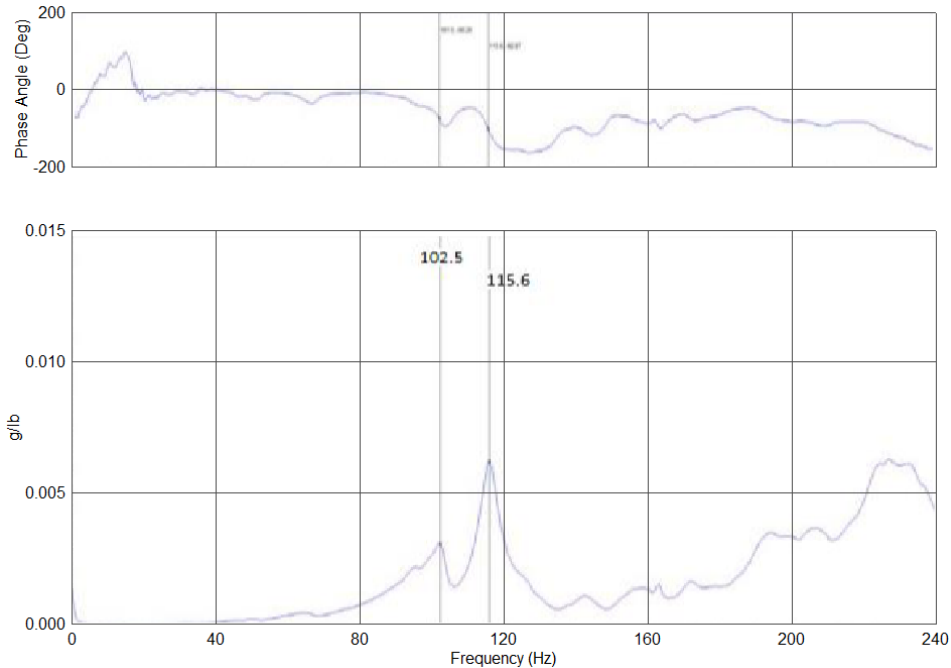


Figure 13. Final Axial Bump Test, DE Bearing Housing

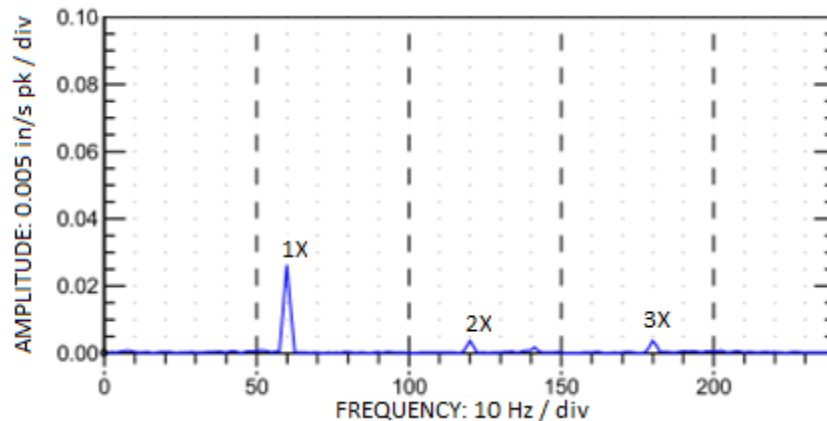


Figure 14. Final Axial Vibration Spectrum, DE Bearing Housing

### ***Summary and Follow-up Considerations***

Considerable effort was invested due to an axial vibration concern on the DE bearing housing, and because of a bump test peak within the 15% SM of the 2× rated line frequency and 2× rated running speed. Extensive analyses and testing of several bracket design combinations to reduce the axial vibration were applied. Multiple attempts were made to correlate test results with the analysis. It was determined that the slightly elevated DE axial vibration relative to the radial was a result of the combination of both bracket and frame response to the 2× electrical line frequency.

In this case study, both the original bearing bracket design, and even the bracket with no stiffeners, would likely have been useable, but lack of understanding of the actual mode shape resulted in more focus being placed on areas of lesser affect. More rigorous testing and analysis of the entire motor frame structure were required to know which modifications would have the highest potential for measurable effect on vibration performance. It is important to note that natural frequencies as provided by bump testing are much more useful if they can be correlated with FEA because this provides a high confidence that the FE model and predictions are accurate. By understanding the mode shape, it can then be determined where to adjust the structural stiffness for the most effective result.

In retrospect the entire process could have been abbreviated by implementation of Operational Deflection Shape (ODS) analyses as opposed to a combination of bump testing, new bracket designs, and FEA studies. ODS offers a means to experimentally capture the actual operational mode shapes that show both natural modes as well as those produced by forcing functions such as electro-magnetic and other dynamic forces as discussed in the next section. Motion amplification video (MAV) is another tool [26] that could be used; however, it may not be appropriate for these higher frequencies near 120 Hz.

**EXAMPLE OF ODS DURING FAT**

Vibration testing was performed on a new motor during the factory acceptance tests (FAT). It was previously noted that the motor bearing housings had natural frequencies near 60 and 120 Hz electrical frequencies that did not meet API 541 recommended SMs. In addition, it was reported that the bearing housing vibration exceeded the API limit of 0.1 ips peak when the motor was operating in the no load, cold condition.

***System Description***

The motor is shown in Figure 15. The motor nameplate information is provided in Table 6.



Figure 15. Motor on Shop Floor

Table 6. Motor Description

Motor Type	Induction (API 541)
Frame Size	1000
Enclosure	WP2
Rating	14,000 HP, 12,470 V, 543 FLA
Full Load Speed	1795 RPM
Service Factor	1.15
Rotation	CCW (as viewed from NDE)
Bearing Type	Sleeve

**Vibration Limits**

The acceptability criteria shown in Figure 16 were used to evaluate the data that were obtained. API Standard 541 for induction motors provides the following (shaft probes for displacement and bearing housing accelerometers for velocity).

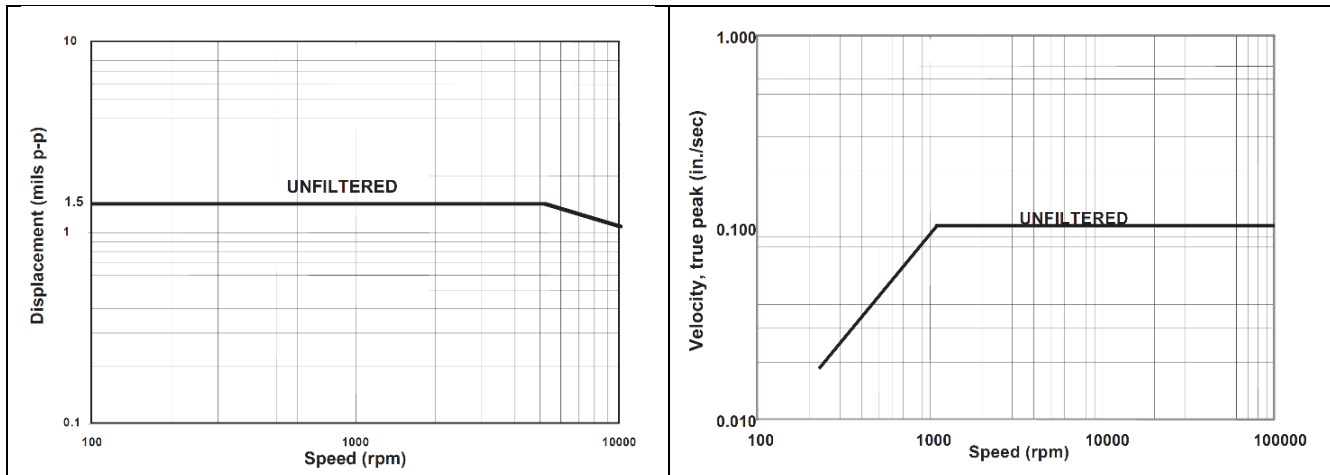


Figure 16. API Vibration Limits

For this motor running near 1800 RPM, the limits are 1.5 mils p-p overall at the shaft proximity probes and 0.1 ips 0-p for bearing housing accelerometers. In addition, API 541 specifies that the no significant resonance shall occur within  $\pm 15\%$  of one and two times running speed,  $\pm 15\%$  of one and two times line frequency, or between 40% and 60% of running speed.

The following sensors were used for the shop test:

- A laser tach was installed at the DE motor shaft for a once-per-revolution signal.
- The existing motor shaft proximity probes were measured and recorded.
- Single-axis accelerometers were magnetically mounted on the motor bearing housings.
- Tri-axial accelerometer was used at various points for the ODS.

**Impact Tests**

Impact tests were performed while the motor was slow rolling near 300 RPM so that the shaft was on the oil film as directed by API 541. Table 7 shows a summary of the natural frequencies.

Table 7. Measured Natural Frequencies (Horizontal and Axial)

Location	Nat. Freq.	SM	AF
NDE Bearing Housing	62.25 Hz	3.8%	14
	67.75 Hz	12.9%	16
	121 Hz	0.8%	10 - 11
DE Bearing Housing	62.5 Hz	4.2%	--
	70 Hz	16.7%	24 - 25
	123.75 Hz	3.1%	11



On the NDE bearing housing, natural frequencies were identified near 62 and 68 Hz. These are within 15% of the 1× electrical frequency (60 Hz). In addition, another natural frequency was identified near 121 Hz, which is within 15% of the 2× electrical frequency (120 Hz).

Figure 17 shows an example of the impact test results on the NDE bearing housing. Frequency response functions (FRF) are shown for all three directions (X=axial, Y=vertical, and Z=horizontal). The response amplitude is normalized to the applied force (g/lb) and averaged over five hammer hits. The phase angle is plotted in degrees above each response. A response peak and phase shift will indicate a natural frequency.

As shown in Figure 17, there was a natural frequency measured at 120.75 Hz in the horizontal and axial directions. A curve fit was used to determine the damping based on the sharpness of the peaks. The calculated amplification factor was 10 - 11, therefore this mode is not considered to be well damped since the AF is well above 2.5. It is also within 1% of the 120 Hz electrical frequency and does not meet the required API separation margin indicated by the red shaded areas.

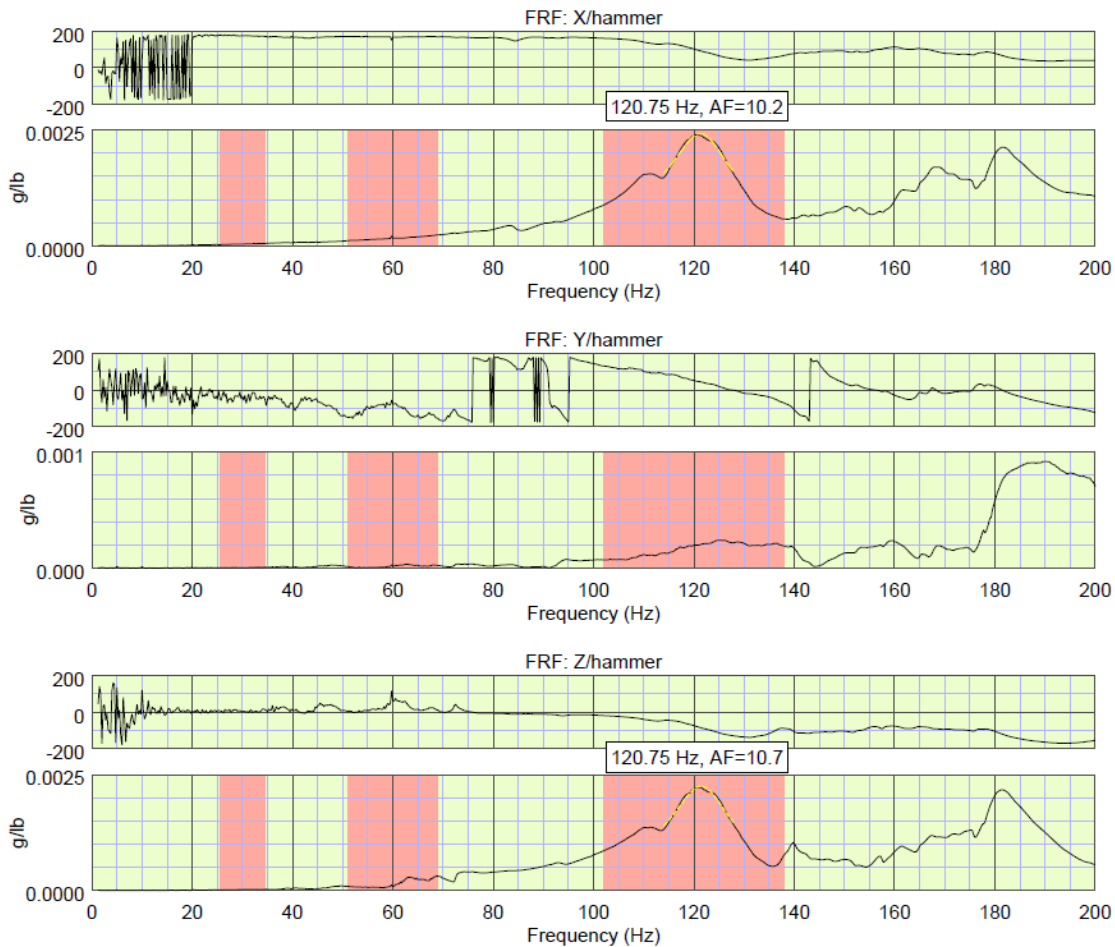


Figure 17. Example of Impact Test Results

On the DE bearing housing, natural frequencies were identified near 62, 70 and 124 Hz. The third natural frequency is within 3% of the 2× electrical frequency (120 Hz) and has AF = 11. The corner of the motor frame was impacted, and the natural frequencies identified on the bearing housings were not evident. This likely indicates local modes of the bearing housings and end bell plate.

The measured natural frequencies of the bearing housings could be amplifying the observed vibration levels. To visualize the motion an ODS was performed. Typically, the motion will approximate the mode shape of nearby natural frequencies.

**Operating Deflection Shape (ODS)**

A geometric model was created of the motor and bearing housings (Figure 18). While the motor was in the hot condition, amplitude and phase data were acquired at multiple locations (numbered). ODS is explained further in reference paper [27].

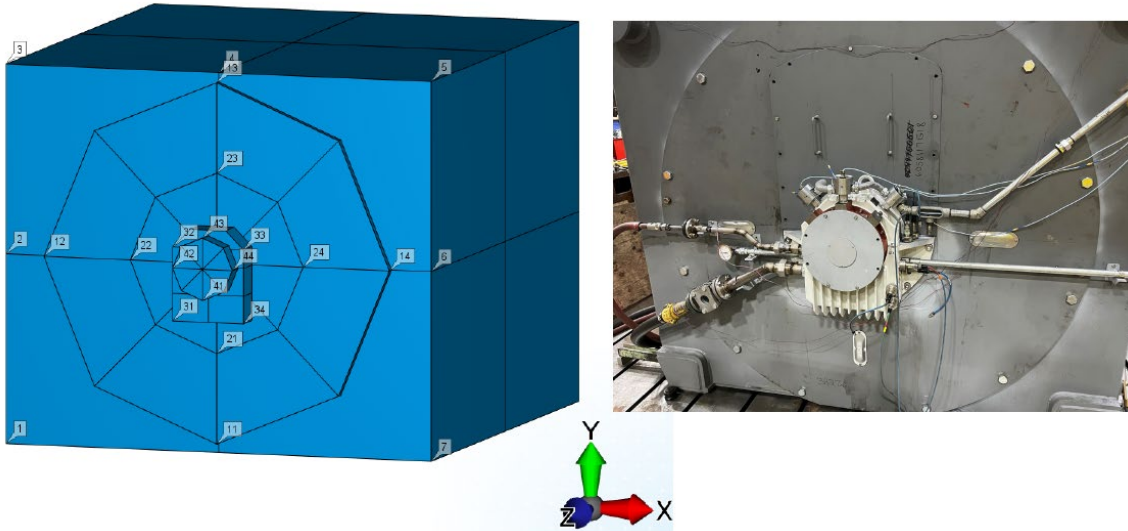


Figure 18. Example of ODS Model and Numbering

As shown in Figure 19, the vibration amplitude at 30 Hz (1× running speed) was low. However, at 60 Hz (1× electrical frequency) the vibration was higher amplitude and at 120 Hz (2× electrical frequency) the vibration was the highest amplitude when plotted in velocity (in/sec). For reference, a velocity reading of 0.08 ips peak converts to a very small displacement of 0.2 mils p-p at 120 Hz.

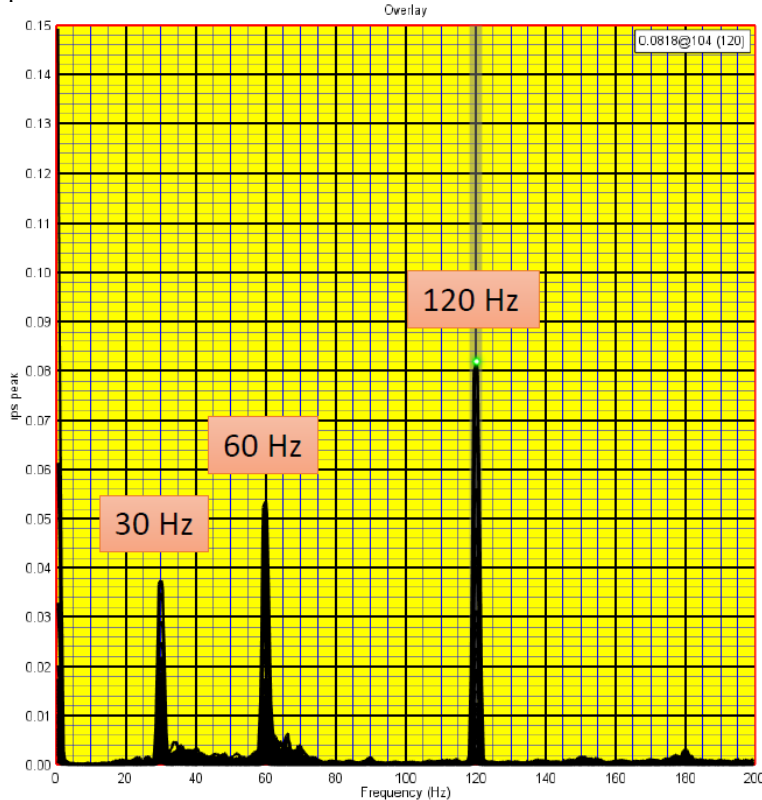


Figure 19. Overlaid Frequency Spectra Plots of All Measurements Taken for ODS

The ODS at 60 Hz shows that the motor bearing housings are moving in the axial “Z” direction and vibrating out-of-phase with each other (Figure 20). The orange arrows indicate axial motion of the bearing housings. The animation for motion at 60 Hz has been embedded into this tutorial. See Figure A.1 of the Appendix to view the animation of the ODS at 60 Hz.

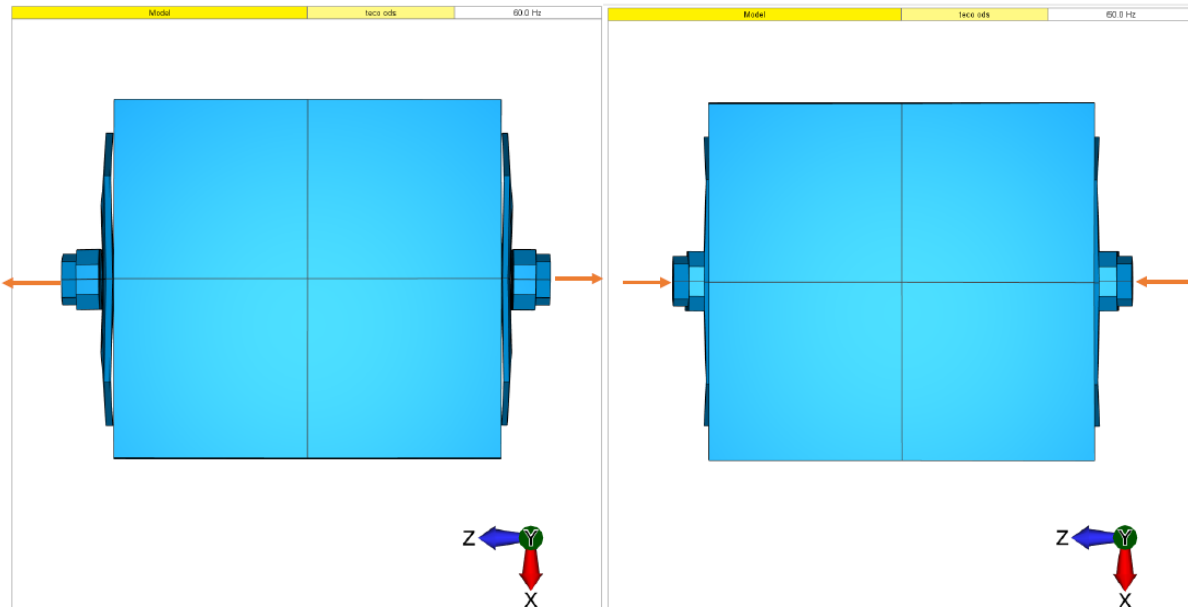


Figure 20. ODS Showing Axial Motion of Bearing Housings at 60 Hz

The ODS at 120 Hz shows that the motor bearing housings are pivoting side-to-side, and the end bell plate is flexing. The motion is in-phase on the DE and NDE bearing housings (Figure 21). The orange arrows indicate motion of the bearing housings in the horizontal “X” direction. The animation at 120 Hz can be viewed in Figure A.2 of the Appendix.

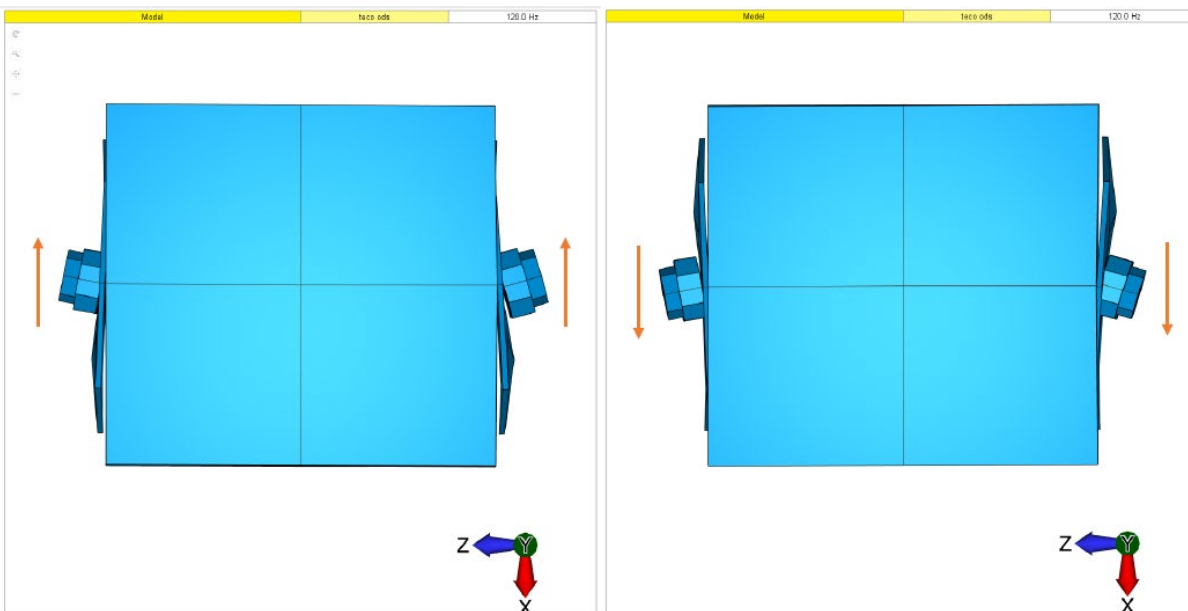


Figure 21. ODS Showing Horizontal Motion of Bearing Housings at 120 Hz

Increased vibration levels can occur when a natural frequency coincides with a multiple of motor running speed or electrical excitation frequency. As will be discussed in the following sections, the excitation at 120 Hz is related to motor voltage and flux.

### ***No Load Test with Cold Motor***

The no load test was performed. The motor was in cold condition at the beginning of the test. Since the motor was unloaded and running across the line with 60 Hz power, the speed remained near 1,800 RPM. The overall vibration levels of the bearing housings were low in the radial directions. However, in the axial direction the vibration levels reached 0.12 ips peak, which exceeds the API limit of 0.1 ips peak. The overall shaft vibration levels were below the API limit of 1.5 mils p-p and considered acceptable.

### ***Voltage Test***

Before shutting the motor down, a test was performed where the voltage was briefly decreased to 90% and then increased to 110% of the rated. The bearing housing vibration at 120 Hz decreased at lower voltage and increased at higher voltage. However, the bearing housing vibration at 30 Hz and 60 Hz were not significantly affected by changing the voltage. In addition, motor shaft vibration was insensitive to the motor voltage. Therefore, it appears that the excitation source is electrical in nature (related to magnetic forces / flux).

### ***Startup and Shutdown***

The shaft vibration levels during startup and shutdown were low. Amplitudes were below 0.5 mil p-p. It was reported that the motor has been balanced in accordance with API (4W/N), which is approximately equivalent to ISO G0.7. The bearing housing vibration was highest in the axial direction, which would not be unbalanced force. Peaks were identified near 60 and 120 Hz, which are the electrical frequencies.

### ***No Load Test with Hot Motor***

Next, a four-hour heat run was performed in which full load amps was simulated with dual frequency operation (50 and 60 Hz). This method is explained in reference papers [28,29]. Vibration readings were not taken during this test since it did not represent realistic operation. At the end, the hot motor was shutdown to check resistance.

The motor was restarted while still hot and operated at no load with the rated voltage at only 60 Hz electrical frequency. The ODS was gathered during this time with the motor hot. Bearing housing vibration was slightly lower, but the shaft vibration levels were higher for the hot motor condition compared to the cold motor condition previously measured.

The overall bearing housing vibration was low in the radial directions. However, in the axial direction the vibration levels were between 0.08 and 0.105 ips peak, which was slightly better than the cold condition, but still near and slightly above the API limit of 0.1 ips peak.

When the voltage was reduced to half value, the vibration levels on the bearing housings dramatically decreased. Axial vibration was less than 0.06 ips peak and radial vibration was 0.02 ips peak. For the overall shaft vibration, three of the proximity probes showed values below the API limit of 1.5 mils p-p. However, the X-probe on the NDE had vibration levels of 1.6 mils p-p, which slightly exceeded the API limit of 1.5 mils p-p for a brief time. Note that the shaft probe readings were insensitive to voltage applied to the motor.

A comparison was made of the shaft vibration in the X-direction on the NDE when the motor was cold versus hot. The vibration amplitude at 1× running speed increased from 0.6 to 1.1 mil p-p indicating increased imbalance possibly due to bowing of the shaft after the hot restart of the motor [30].

### ***Summary and Follow-up Considerations***

The test results matched mode shapes predicted by the finite element model of the motor. However, the natural frequencies were slightly different. The FE model can be normalized to match the measured results. Stiffeners could be added to the existing end bell plates and/or use thicker end bell plates to detune these natural frequencies in the model. Preliminary FEA results showed an increase in the natural frequency was possible. The end user decided not to accept the motor and the end bells (i.e., *bearing brackets*) were redesigned so that the motor complied with API vibration limits before shipment.

As in the previous critical speed and vibration case study of the 2-pole motor, this is another example where extensive analysis and testing were required to pinpoint the exact mode shapes and frequencies of the offending vibration, which again, was largely a result of the 120 Hz electrical forcing frequency corresponding relatively close to a structural resonance. In this former case it was initially assumed, although incorrectly, that the bearing brackets were the problem, but in this case, both the FEA and ODS were implemented much sooner in the process and were able to identify frequencies and deflections in the bearing brackets. This consequently allowed the further use of FEA to design a bracket modification that proved effective.

The question, of course, is, could these post-manufacturing modifications have been avoided by implementation of more robust up-front design practices and procedures? The answer: “Maybe.” In the design of large *custom* products, one best practice is to use equivalent, or near equivalent, references wherever possible. The key word here is “custom.” Using a proven reference design is always a good starting point but can never guarantee success in every measure. Custom designed motors with special mounting patterns, offset cores, core lengths, flux densities, air gaps, structural differences, critical speeds, and differing bearing sizes, etc. can all influence vibration performance. A slight deviation from a specification usually does not mean a machine has a systemic defect, but it may be difficult to convince a user to allow a deviation from an industry standard, no matter how small. Some of the challenges faced by the motor designer are:

- 1) Prediction of how much vibratory response the machine will have to the  $2\times$  excitation frequency. The magnitude of the  $2\times$  excitation will vary from one design to the next based on differences in design flux densities, back-iron depth, stacking pressure tolerances, core lengths, structural resonances, and other variables. Each case is different. Incorporation of best-known methods, design limits, checklists, experience, and consistent careful manufacturing practices can minimize the risk. In this example it was believed that all the best practices had been followed, and in fact the machine performed very well except that one axial vibration reading was periodically slightly out of tolerance.
- 2) Pre-determination of whether to conduct a FEA. This can be expensive, extensive, time consuming and results can vary significantly depending on boundary conditions and other assumptions. With accurate 3D models, interface treatments, and force inputs, structural resonances can be largely avoided as proficiency and experience increase.
- 3) Identification of appropriate test measures needed to identify and isolate the problem. When deviations do occur that are not easily identified by prior analysis, it can save a lot of time by using proven test methods, such as ODS, to develop solutions in the shortest possible and least costly time frame, as was the case in this example.
- 4) Understanding of the governing specifications and where possible exceptions should be taken and why. It is much easier to take any needed exceptions to specifications at the time of the negotiation than to obtain a concession after manufacture and factory acceptance test.

## **DISCUSSION ON VIBRATION LIMITS AND STRUCTURAL RESONANCES**

Everyone agrees that it is best for vibration levels to be minimized whenever possible. However, the continued evolution of industry standards relative to allowable vibration levels and structural resonances combined with the increased need to operate over wide speed ranges can be problematic. These all contribute to more restrictions on designs and more opportunities for non-compliance. Therefore, the following discussion is warranted to help justify and explain possible deviations when they occur.

1. Do peak(s) in the vibration spectrum data indicate that a corresponding structural resonance is present nearby?
2. Is a structural resonance near an excitation frequency a reliable predictor of a problem or potential future problem?
3. What is the relative importance of shaft vibration, bearing housing vibration, and frame skin vibration?
4. What is the relative importance of axial versus radial vibration?
5. Is the API bearing housing natural frequency test a reliable indicator of a potential problem?

### ***Peaks in vibration spectra related to structural resonances***

A peak in the vibration spectrum does not necessarily mean there is a structural resonance present, but it does indicate a forcing function at that frequency. A resonant condition will amplify the response to a forcing function. Therefore, a peak that corresponds with a structural resonance can result in high vibration levels. An unacceptable level of response is one that generally exceeds a published vibration limit, causes excessive noise, or is perceived to be a long-term stress or fatigue concern.

It is usually difficult to totally eliminate a peak in the vibration spectrum, although many times the magnitude can be reduced by changing the system stiffness, adding damping to the system, and/or decreasing the strength of the forcing function. These changes, when possible, can affect the magnitude and amplification factor but generally cannot eliminate the response completely. Forcing functions are usually, but not always, systemic in the design to some degree and can normally be predicted or identified if not caused by some unknown defect. When the forcing function is a well-known phenomenon, experience and judgment should be part of the evaluation process.

A common forcing function in rotating equipment is imbalance. This is a once-per-revolution ( $1\times$ ) peak will exist since balancing to perfection is not possible. Another common forcing function is the twice-per-revolution peak generally caused



by out-of-round journals, misalignment, or, in the case of two and four-pole machines,  $2\times$  line frequency. There are other sources of vibratory peaks and most vibration literature related to vibration diagnostics of rotating equipment will provide extensive lists of potential forcing phenomenon, their sources, and their frequency(s) relative to running speed.

The purpose here is to determine if the peak corresponds with a resonance in the system and whether or not the condition constitutes a problem. Therefore, once a peak is identified that is perceived as a concern, the following steps should be considered:

#### *Identify the cause of the forcing function*

As mentioned above, most vibration diagnostic literature will provide the most common forcing phenomenon causes. One common example is the  $2\times$  line frequency (120 Hz). This is a common peak in the vibration spectrum and can be confirmed as the cause by monitoring vibration and temporarily reducing or cutting the supply voltage.

#### *Evaluate potential ways to influence the forcing function*

Determine if it can be eliminated or reduced. Examples include improving the balance, adjusting the air gap, eccentricity, checking the alignment, consideration of external influences (i.e., surrounding equipment), reducing thermal distortion or loading, uneven cooling, machining the journals, checking mounting conditions (i.e., soft foot), critical speed check, broken rotor bar check, bearing inspection, reducing the supply voltage (if possible), etc.

#### *Check for natural frequencies*

A peak does not mean the existence of a resonance, but a resonance can greatly amplify the magnitude of the peak. Detection of a resonance usually requires variable speed run and/or a bump test in which the structure is checked at or near the same location and direction as the vibratory peak. A properly performed bump test will excite all predominate natural frequencies and the data can then be correlated with the vibration spectrum. A resonant peak in the proximity of the vibration peak (typically within 5%-10%) can generally be assumed to be excited by the corresponding forcing function.

Other methods for detecting resonances are run-up/coast-down, shaker tests, electromagnetic exciters, and noise floor analysis. Once a natural frequency is found, the magnitude, damping, and proximity to a forcing function frequency must be evaluated at that point. Note that shaft displacement is a relative measurement (shaft to housing). Therefore, significant housing vibration could affect the meaning of the measured shaft displacement. Housing vibration will be discussed further in a following section.

A quality FEA may be used to evaluate the amount of mass modal participation for the mode in question. Modal participation measures the amount of mass moving in each direction for each mode. For example, if the mode being evaluated shows axial movement but low mass participation in the axial direction, it means not much of the structural mass is participating in that direction. This is one way to justify that an excitation corresponding to a particular resonance to be of low risk since modes with low effective masses cannot be easily excited. Other options are to find methods to reduce or eliminate the corresponding forcing function(s) through precision balancing, etc.

#### ***Relative importance of shaft, frame, and bearing housing vibration***

Most industry standards have limits on allowable shaft and bearing housing vibration, but more recently restrictions have been imposed on the frame structure by some standards. Since the frame, shaft, and bearings are the three major components of the system it makes sense to consider what guidelines may be used to impose reasonable limits.

Frame vibration collected on the test floor on the machine centerline and in line with a bulkhead or stiffener as required by API gives an overall “feel” for the stiffness of the structure. A high frame vibration will usually manifest as high vibration on the bearing housings or higher-than-normal noise. Frame vibration information is useful when attempting to diagnose other out-of-tolerance conditions or justify more detailed analysis or testing. Another consideration is the frame skin vibration. Large unsupported spans of frame skin can result in localized resonances that add energy to the entire structure and show up as a peak in a bump test result of an unrelated component, such as a bearing bracket for example. The case study in this paper describes a frame rocking mode that was initially interpreted as a bearing bracket resonance.

The rotating element, shaft/rotor, is typically the major driver for vibration due to the dynamic forces produced, primarily by unbalance or torque pulsations, especially when operating near a lateral or torsional critical speed. Rotors on induction motors, for example, are of generally very robust construction, but high radial or torsional vibration can cause long term fatigue to components like rotor bar braze joints, fan blades, and bearings. Synchronous machines, on the other hand, may

have control wheels with resistors and other electronic components. However, they also usually run at much slower speeds, which means the dynamic forces are usually low.

Another very important consideration is that of both the coupling and driven equipment. Since the rotor is coupled to the driven equipment, it follows that shaft vibration evaluation should be done in the uncoupled condition when possible and also take into consideration the unbalance of any half coupling that may remain on the shaft. The half coupling weight usually does not affect the first lateral critical speed but could influence the second lateral critical speed.

It is safe to say that the shaft vibration limits provided by industry standards have in general proven very reliable and reasonable due to the many years of experience and scrutiny by experts in this field. Shaft vibration is usually measured in units of displacement whenever possible since displacement can be compared directly to bearing and other internal clearances as well as recommendations from the manufacturer. Note that shaft displacement is a relative measurement (shaft to housing).

It is also important to make a distinction between initial factory acceptance testing (FAT) and field operation. API 541, for example, has filtered and unfiltered vibration limits, as well as vector shift and residual unbalance criteria which are designed to be imposed during factory acceptance testing of the machine when mounted uncoupled on a massive foundation. End users typically will have their own well established vibration limits based on statistical data and operating experience.

Bearings and bearing housings support the rotor, which means much of the rotor vibratory energy will be transmitted to, and through, the bearing housings to the surrounding structure. Some of the rotor energy will be attenuated and dampened by the sleeve bearing oil film, which is one of the benefits of using hydrodynamic bearings. The bearing housing vibration is still a reliable indicator of the rotor condition since the bearings are the interface between the frame and rotating element, which means bearing housing vibration is a result of forces imposed by both the rotor and frame. Frame forces are produced by the radial and torsional magnetic interaction between the stator and rotor, and also that which is transmitted through the mounting structure or other interfaces. It is therefore very important to minimize or eliminate any external vibration sources when evaluating the health of a machine using bearing housing vibration data.

The purpose of the vibration alarm and shutdown limits is to improve reliability, prevent further damage, and avoid a possible safety incident. However, when attempting to bring a machine into compliance or evaluate whether to accept and operate a machine with a slight out-of-tolerance condition, knowing the major contributors to the overall can be extremely important.

If it were assumed the vibration sources were known and subsequently confirmed there was nothing additional that could be done (within reason) to reduce or eliminate these sources, would, or should, this be of concern to the user? The answer is based on whether the consequences of these other contributors to the vibration would potentially be a problem, which means one must understand what the long-term affect would be. Vibration is composed of both displacement and frequency.

Displacement can be an issue when considering bearing clearances, which is why shaft vibration is typically measured in units of displacement as mentioned previously. Overall shaft vibration under 50% of the diametrical bearing clearance would not be expected to damage the babbitt. The frequency of the displacement can cause fatigue if combined with high amplitudes, and sometimes cause noise issues as well. Subsynchronous vibration could be an indicator of additional problems, rubbing, etc.

The bearing housing vibration is typically measured in units of velocity (inches-per-second). If it could be determined that neither the displacement nor the frequency of the housing vibration would cause a problem as related to fatigue or running clearances, then there is little risk in operating the machine as is. Unless high-frequency buzzing occurs that could loosen bolted joints, etc.

Displacement typically must be of sufficient magnitude to cause an impact, rub, or high stress in the structure. Impacts can cause immediate damage and/or excite other natural frequencies. High oscillating stresses can cause fatigue. If the displacement component is small then the frequency will have little, if any effect on long-term reliability, simply because there will be no stresses anywhere near the fatigue strength of the structure. If a vibration frequency is close to a structural resonant frequency, then it will take less energy to produce higher vibration, which may cause an out-of-tolerance condition, but this may be of negligible consequence for the reasons discussed—namely because the magnitude, noise, or modal mass participation are still well below the threshold where they can do harm.

### ***Relative importance of axial versus radial vibration***

Another important consideration is the direction of the vibration being measured, which brings up an interesting point: Sleeve bearing machines are typically coupled to driven equipment through limited end float couplings designed to limit allowable axial shaft travel to a value (typically +/- 0.095 inch as per NEMA [31]) that is much less than the axial clearance allowed by the sleeve bearings (typically +/- 0.25 inch).

This begs the question of why axial vibration on the bearing housings of sleeve bearing machines is limited to values at least one or two orders of magnitude less than that which the coupling will allow the shaft to move relative to the housing. For example, the typical housing axial vibration limit imposed during factory acceptance is 0.1 ips 0-p, and for an 1800 RPM machine this converts to +/-0.001 inch (i.e., 1 mil p-p) displacement if assumed to only be comprised of the 1× component. This is not to suggest, however, that axial vibration limits be increased to the point of being restricted by the coupling end float tolerance, but to show that there can be justification to allow higher lenience for axial vibration relative to radial. However, any allowed increase must not allow bumping against a bearing thrust face or coupling stop, as this could excite other natural frequencies in the system or drive train.

It is understood that an axially mounted transducer on the bearing housing may well be detecting vibration coming from sources and deflections that are not purely axial, so to some degree it makes sense that axial vibration should be minimized. However, it is also justifiable to consider that in sleeve bearing applications there is potentially a much higher tolerance for axial motion on the bearing housing since there is little ability to transmit the axial motion across the oil film.

Sometimes industry standards provide different limits as a function of the vibration direction as related to the type of bearings being used. In this case study the limits were imposed by API 541, which currently does not give different limits as a function of vibration direction or bearing type but are based on motor speed only. From a technical standpoint the motor in this case study was in compliance at rated speed, but due to machine size and rotordynamic performance requirements the vibration performance was subjected to extra scrutiny. Since the axial vibration was considerably higher than the radial, the steps previously described were used to further reduce the axial component.

Axial vibration is more likely to include higher frequency components because bearing housing vibration is affected by other forcing functions besides the radial unbalance of the rotor. This is why it is not uncommon for axial vibration readings to be considerably different than radial. One likely reason in the context of electrical machinery is that the 2× line frequency typically manifests as axial vibration, especially on two and four-pole machines where the radial magnetic forces are higher relative to the effective stiffness of the stator and frame. The radial 2× vibration frequency essentially compresses and expands the stator core structure slightly due to the rotating magnetic field. The stator is tied to the core bulkheads, and radial vibration in the core bulkheads is transmitted to the end bulkheads via the frame skin and any stiffeners which connect the inner and outer bulkheads. Therefore, radial motion on the core bulkheads can manifest as axial vibration on the outer bulkheads to which the bearings brackets (i.e., “end bells”) are attached.

Sleeve bearing machines usually have higher tolerance for axial vibration on bearing housings and surrounding structures because there are no mechanical limitations imposed in the axial direction. This is due to the allowable endplay between the shaft shoulders and bearing journals being orders of magnitude higher than the actual axial movement due to vibration. The only interface between the bearing and shaft is the oil film and therefore axial motion is limited only by the stiffness of the support structure. Small axial vibration excursions therefore have no measurable negative consequence to the life, performance, or reliability of the rotor or bearings because there is little to no ability for axial vibration on the bearing housing to transfer across the oil film of the sleeve bearings to affect the rotor as previously stated. Because of these factors, higher axial vibration, therefore, can generally be considered more tolerable on sleeve bearing machines relative to radial, and this should be considered when dealing with machine evaluation.

There are always exceptions of course. Some machines may have special bearings designed to absorb axial thrust and therefore have small axial clearance. These would have more potential for damage from high axial housing vibration. Another consideration is that, although an out-of-tolerance axial vibration may be due to a high frequency component, one should confirm not only the frequency, but the underlying cause. While there may be little that can be done to reduce the 120 Hz electrically induced vibration after a machine has been built, it must be noted that high frequency contributions can also be due to out-of-round journals, bad air gaps, broken rotor bars, looseness, etc., which must be identified and corrected.

### ***API bearing housing natural frequency test reliability and usefulness***

The bearing housing natural frequency test in API 541 is as follows:

*When specified, bearing housings or end bracket supports shall be checked for resonance on one fully assembled machine of each group of identical machines. The resulting response shall be plotted for a frequency sweep of 0% to 400% of line frequency. In order to eliminate the interaction between the bearing housings, the rotor shall be turned at a slow roll (200 to 300 RPM). The response plots shall be made on each bearing housing in the horizontal, vertical, and axial directions. The application of the excitation force shall be made in these same directions.*

*No significant resonance shall occur within  $\pm 15\%$  of one and two times running speed,  $\pm 15\%$  of one and two times line frequency, or between 40% and 60% of running speed as required by 4.4.2.1. A significant resonance is defined as a peak that lies within 6 dB in amplitude (displacement) of the fundamental bearing housing resonance in the particular direction being tested. Percentages are based upon one times running speed and electric line frequency.*

The goal of the subject test is to check for resonant conditions of the bearing housing or support bracket that lie within the frequency bands given. It is believed that resonances within these bands can result in out-of-tolerance vibration levels. After many years of conducting these tests, however, experience has shown that a significant number of machines do not, or would not, comply, but still meet the API 541 vibration limits and have not had long term issues with vibrations. This seems to confirm API 541 note 7-32 which states:

*Bearing Housing Natural Frequency Test - Normally specified for the first motor manufactured of a certain frame size or a uniquely designed motor. The risk of not requiring the test is low due to the low bearing housing vibration limits required by API 541, and if the motor passes the vibration tests, the motor probably does not have a significant resonance.*

## **CONCLUSIONS**

As discussed in this tutorial, two-pole motors can produce higher magnetic forces and possible vibration compared to four-pole motors. While using a VFD can offer a wide speed range, it could also increase the chances of encountering a natural frequency. Building a new motor to fit within an existing space to replace an old motor can present challenges. All of these factors should be considered in the design stage.

This tutorial showed the critical features needed to produce a large motor capable of a broad speed range by optimizing shaft and core stiffness, bearing type and size, bearing supports and frame structure. The result was a design where non-critically damped peaks were well outside the operating range and “peaks” within the operating range were critically damped. Subsequent testing raised questions about the relative importance of the different types of vibration and the measurement directions and magnitudes, which were each discussed.

While it is understood that low vibration and avoidance of structural resonances is the goal, practical considerations can make these difficult to achieve in many cases, especially in the field. This tutorial provided items to consider during negotiation, design, factory testing, and subsequent acceptance or rejection of a machine based on vibration levels and resonances. Finite element analysis and operating deflection shape are two tools available for further evaluation.

An overview of the FAT was presented with vibration measurement technics such as impact testing and ODS. The animation can be helpful in comparing with FEA results to understand the mode shape of the motor frame or bearing housing. Finally, it is suggested that API update the motor standard to differentiate between radial and axial vibration, especially on bearing housings.

## NOMENCLATURE

AF	= amplification factor
API	= American Petroleum Institute
AFD	= adjustable frequency drive
ASD	= adjustable speed drive
CPM	= cycles per minute
D	= shaft diameter (in)
DE	= drive end
E	= Young's Modulus (psi)
FAT	= factory acceptance test
FEA	= finite element analysis
FRF	= frequency response function
$f_1$	= first natural frequency of the beam (Hz)
$f_r$	= rigid bearing critical (Hz)
HP	= horsepower
Hz	= Hertz (cycles per second)
ID	= inside diameter
ips	= inches per second
$K_b$	= bearing stiffness (lb/in)
$K_s$	= shaft stiffness (lb/in)
L	= shaft length (in)
LNG	= liquified natural gas
mil	= 0.001 inch
N	= operating speed (RPM)
NDE	= non-drive end
$N_{c1}$	= first critical speed of rotor
$N_1$	= initial speed at $0.707 \times$ peak amplitude
$N_2$	= final speed at $0.707 \times$ peak amplitude
NEMA	= National Electrical Manufacturers Association
OD	= outside diameter
ODS	= operating deflection shape
peak	= same as zero-peak amplitude, commonly used for vibration in ips and g's
p-p	= peak-to-peak or twice amplitude, commonly used for vibration in mils
RPM	= revolutions per minute
VFD	= variable frequency drive
VSD	= variable speed drive
$W_m$	= modal weight (lb)
0-p	= zero-peak amplitude commonly used for ips and g's

## APPENDIX

Vibration amplitude and phase data were acquired at multiple locations and applied to a geometric model of the motor frame and bearing housings. Operating deflection shape (ODS) animations were created using software from Clear Motion Systems and embedded into this Appendix.

Figures A.1 and A.2 show the ODS animation of the motor at 60 Hz and 120 Hz ( $1\times$  and  $2\times$  running speed), respectively. Note to view these animations within Adobe Acrobat "trust" the document under the options bubble, and then click the red question mark in the top left corner. Once activated, the animation should start. Buttons in the toolbar can be used to rotate or zoom the geometric representation of the motor.



Model / ODS / 60.0 Hz

Figure A.1 - ODS Animation at 60 Hz

Model / ODS / 120.0 Hz

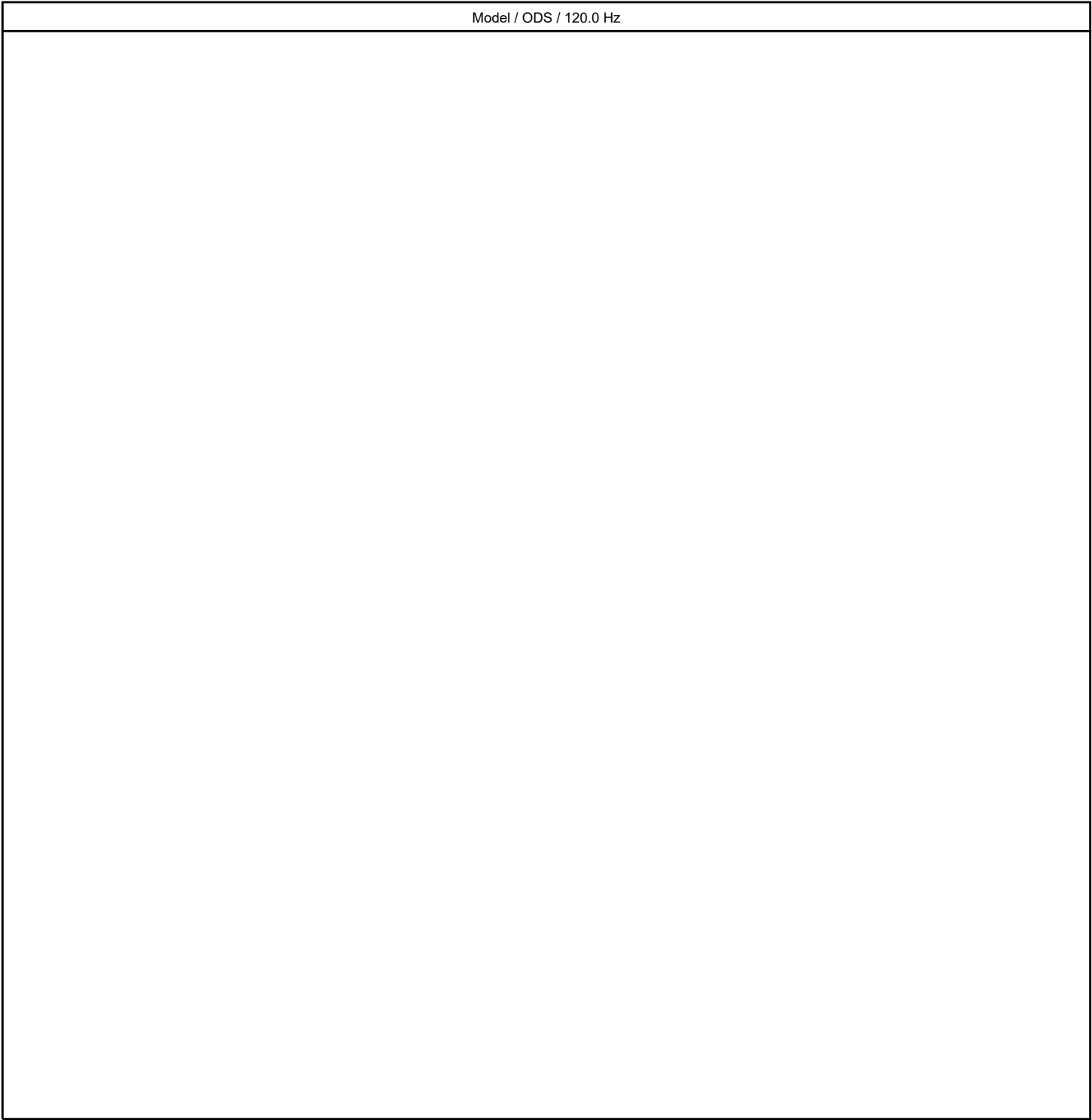


Figure A.2 - ODS Animation at 120 Hz

## REFERENCES

- [1] Donner, G., Subler, B., Evon, S. "A Motor Primer (Part 1)," PCIC-99-28, 1999.
- [2] Donner, G., Subler, B., Evon, S. "A Motor Primer (Part 2)," PCIC-2001-29, 2001.
- [3] Donner, G., Oakes, B., Evon, S. "A Motor Primer (Part 3)," *IEEE Transactions of Industry Applications*, Vol. 39, No. 5, September/October 2003.
- [4] Oakes, B., Donner, G., Evon, S. "A Motor Primer (Part 4)," *IEEE Transactions of Industry Applications*, Vol. 40, No. 5, September/October 2004.
- [5] Oakes, B., Donner, G., Evon, S., Paschall, T. "A Motor Primer (Part 5)," *IEEE Transactions of Industry Applications*, Vol. 43, No. 3, May/June 2007.
- [6] Finley, W., Hodowanec, M., Holter, W. "An Analytical Approach to Solving Motor Vibration Problems," PCIC-99-20, 1999.
- [7] Feese, T., Schnitzler, W. "Special Considerations for Electric Motors Driving Reciprocating Compressors," Gas Machinery Conference (GMC), Louisville, Kentucky, 2021.
- [8] Corey, Cletus A. "Review of Fundamental Two Pole Induction Motor Mechanics." *Proceedings of the 14th Turbomachinery Symposium*. Texas A&M University. Turbomachinery Laboratories, 1985.
- [9] Miller, William H. "Large Motor Specification and Selection." *Proceedings of the 17th Turbomachinery Symposium*. Texas A&M University. Turbomachinery Laboratories, 1988.
- [10] Costello, Michael J. "Understanding The Vibration Forces In Induction Motors." *Proceedings of the 19th Turbomachinery Symposium*. Texas A&M University. Turbomachinery Laboratories, 1990.
- [11] Thornton, Edward J., and J. Kirk Armitor. "The fundamentals of AC electric induction motor design and application." *Proceedings of the 20th International Pump Users Symposium*. Texas A&M University. Turbomachinery Laboratories, 2003.
- [12] Chen, Edward, Robert Glover, and Bryan Evans. "Using Finite Element Analysis (FEA) To Estimate Reed Frequency of Vertical Motors for Pump Applications." *Proceedings of the 32nd International Pump Users Symposium*. Turbomachinery Laboratories, Texas A&M Engineering Experiment Station, 2016.
- [13] Rama, John C., and Miles Griggs. "High Speed Electric Drive Applications-An Overview." *Proceedings of the 26th Turbomachinery Symposium*. Texas A&M University. Turbomachinery Laboratories, 1997.
- [14] Gilon, Dominique C., and Louis Boutriau. "Experience With High Speed Induction Motors For Direct Driving of Compressors." *Proceedings of the 27th Turbomachinery Symposium*. Texas A&M University. Turbomachinery Laboratories, 1998.
- [15] Holopainen, Timo P., Olli Liukkonen, and Pieder Jörg. "Comparison Of Two-And Four-Pole VSD Motors Up To 4000 RPM." *Proceedings of the 45th Turbomachinery Symposium*. Turbomachinery Laboratories, Texas A&M Engineering Experiment Station, 2016.
- [16] Meucci, Francesco, et al. "The Importance of Structural Modal Analysis in 2 Poles Induction Motors for LNG Application." *Asia Turbomachinery & Pump Symposium. 2016 Proceedings*. Turbomachinery Laboratories, Texas A&M Engineering Experiment Station, 2016.
- [17] API Standard 541, *Form-wound Squirrel-Cage Induction Motors-500 Horsepower and Larger*, Fifth Edition, American Petroleum Institute.
- [18] API Technical Report (TR) 684, *Rotordynamic Tutorial: Lateral Critical Speeds, Unbalance Response, Stability, Train Torsionals, and Rotor Balancing*, American Petroleum Institute.
- [19] Gunter, E. J. "INTRODUCTION TO ROTOR DYNAMICS - Critical Speed and Unbalance Response Analysis," RODYN, October 2001.
- [20] Leader, M. E. "Understanding Journal Bearings," *Vibration Institute Annual Conference Proceedings*, 2012.
- [21] Owen, E. L. "Flexible Shaft Versus Rigid Shaft Electric Machines for Petroleum and Chemical Plants," *IEEE Transactions on Industry Applications*, 2, pp. 245-253, March-April 1991.
- [22] Leader, M. E. "Rotordynamics of Semi-Rigid and Overhung Turbomachinery." *Proceedings*. Vol. 28. Vibration Institute, 2004.
- [23] Chen, W. J. "Energy analysis to the design of rotor-bearing systems." *Turbo Expo: Power for Land, Sea, and Air*. Vol. 78828, 95-GT-314, American Society of Mechanical Engineers (ASME), 1995.
- [24] Seminar Manual, *Rotordynamics of Rotating Machinery*, self-published by Engineering Dynamics Incorporated, [www.engdyn.com](http://www.engdyn.com).
- [25] Jeffcott, H. H. "The lateral vibration of loaded shafts in the neighbourhood of a whirling speed—The effect of want of balance, The London, Edinburgh, and Dublin Philosophical Magazine and Journal of Science." (1919): 304-314.

- [26] Price, Stephen M. “A comparison of Operating Deflection Shape and Motion Amplification Video Techniques for Vibration Analysis.” Asia Turbomachinery & Pump Symposium. 2022 Proceedings. Turbomachinery Laboratory, Texas A&M Engineering Experiment Station, 2022.
- [27] Silva, Ramón A., and Kyle J. Kuecker. “Tips for Troubleshooting with the Operating Deflection Shape (ODS) Technique.” *Proceedings of the 44th Turbomachinery Symposium*. Turbomachinery Laboratories, Texas A&M Engineering Experiment Station, 2015.
- [28] Portos, Javier, and Sandra Tumer. “Equivalent load test for large induction machines—the three-step method.” Fifty-First Annual Conference 2004 Petroleum and Chemical Industry Technical Conference, 2004. IEEE, 2004.
- [29] IEEE Standard Test Procedure for Polyphase Induction Motors and Generators, December 2017.
- [30] Feese, Troy D., and Phillip E. Grazier. “Balance This! Case Histories from Difficult Balance Jobs.” *Proceedings of the 33rd Turbomachinery Symposium*. Texas A&M University. Turbomachinery Laboratories, 2004.
- [31] NEMA MG1 Section 20.29.2. 2016.

## BIBLIOGRAPHY

Nicholas, J. C. “Operating Turbomachinery On Or Near The Second Critical Speed In Accordance With API Specifications.” Proceedings of the 18th Turbomachinery Symposium. Texas A&M University. Turbomachinery Laboratories, 1989.

Singhal, Sumit, Kumar Vikram Singh, and Andrew Hyder. “Effect of laminated core on rotor mode shape of large high speed induction motor.” 2011 IEEE International Electric Machines & Drives Conference (IEMDC). IEEE, 2011.

Singhal, Sumit. “Method of tuning bending and torsion stiffness of ducted rotor core of an induction motor.” U.S. Patent No. 8,319,380. 27 Nov. 2012, Siemens patent [US 2011/0074242](#).

Mistry, Raj, et al. “Influencing factors on motor vibration & rotor critical speed in design, test and field applications.” 2014 IEEE Petroleum and Chemical Industry Technical Conference (PCIC). IEEE, 2014.

Tsytkin, Mikhail. “Vibration of induction motors operating with variable frequency drives—A practical experience.” 2014 IEEE 28th Convention of Electrical & Electronics Engineers in Israel (IEEEI). IEEE, 2014.

J. Dias, A. P. de Carvalho and T. Milani Dietrich, “Design and Testing of Large 2 Pole Variable Speed Pump Motors with Well Damped Rotor Natural Frequency,” 2019 IEEE Petroleum and Chemical Industry Committee Conference (PCIC), Vancouver, BC, Canada, 2019, pp. 397-404, doi: 10.1109/PCIC30934.2019.9074530.

## ACKNOWLEDGEMENTS

The authors would like to acknowledge the time and effort invested by the TWMC test floor and manufacturing personnel to set up, disassemble, modify, reassemble, test, and collect the data during these case studies, as well as the helpful technical input and suggestions. The authors also thank EDI for their support of this tutorial.